THE LIGHT FIELD IN NATURAL SCENES

A.A. Muryy

The layout of this thesis is based on a LaTeX style file written by Wouter
Bergmann Tiest.

THE LIGHT FIELD IN NATURAL SCENES

Proefschrift

ter verkrijging van de graad van doctor
aan de Technische Universiteit Delft,
op gezag van de Rector Magnificus prof. dr. ir. J.T. Fokkema,
voorzitter van het College voor Promoties
in het openbaar te verdedigen op maandag 6 april 2009 om 12.30 uur

door Alexander Alexeevich MURYY

Master of Science in Applied Mathematics,
Far Easter State Transport University
geboren te Khabarovsk, USSR

Dit proefschrift is goedgekeurd door de promotoren:

Prof. dr. H. de Ridder

Prof. dr. J.J. Koenderink

Copromotor

Dr. S.C. Pont

Samenstelling promotiecommissie:

Rector Magnificus, voorzitter

Prof. dr. H. de Ridder, Technische Universiteit Delft, promotor

Prof. dr. J.J. Koenderink, Universiteit Utrecht, promotor

Dr. S.C. Pont, Technische Universiteit Delft, copromotor

Prof. dr. ir. F.W. Jansen, Technische Universiteit Delft

Prof. dr. T.M. de Jong, Technische Universiteit Delft

Prof. dr. P.N. Belhumeur, Columbia University, USA

Dr. R.W. Fleming, Max Planck Institute for Biological Cybernetics, Germany

CONTENTS

CHAPTER 1

INTRODUCTION

All visual information available to the viewer, whether a human observer or a photo-camera, is nothing but a pattern of light, either emitted by primary light sources or reflected off the materials in the scene. The physical processes which underly the interactions between light and scene are extremely complex, which makes the structure of the luminous environment very hard to parse. In order to describe the plenoptics (E. H. Adelson and J. Bergen, 'The plenoptic function and the elements of early vision', 1991) of the scene one has to know the primary illumination, the structure of the scene and the scattering properties of the materials.

The focus of this thesis will be directed to the structure of the light field in natural scenes. More specifically I will address the issue of the structure of light fields in common indoor and outdoor environments and the consequences for object appearance. The theory of the light field (A. Gershun, 'The light field', 1939) has not been extended essentially since 1939 and there is definitely room for improvement.

One of the goals of this thesis is to bridge the gap between the artistic intuition of the notion of the *'quality of light'* and formal scientific descriptions of illumination. I will derive intuitive descriptions of the qualitative, form-revealing effect of light that at the same time have well defined physical meanings. Another important aspect of my research is the spatial structure of the light field in 3D space. Illumination changes spatially from point to point and its behavior depends on many factors. The scattered part of the light is determined by the structure of the scene and the reflective properties of materials, therefore the structure of the light field depends critically on the structure of the scene.

Current light measurement techniques in the area of illumination engineering do not provide sufficient information about the quality of light in 3D spaces. In this thesis we develop a method to measure the lower order properties of light fields and a method to calculate these for the entire space of the scene. We also address the question of the possible generic topological structures of the light field in the empty space in a scene.

1.1 The Light Field

The issue of interaction between the light and the scene first emerged in the area of art. In order to predict the appearance of a scene due to certain illumination conditions painters had to understand the form-revealing effect of light very well. Leonardo was one of the pioneers who started to scientifically study the formation of shading and shadows on objects' surfaces (see Figure 1.1) and other optical effects such as translucency and

Figure 1.1: A schematic drawing of a human head by Leonardo. The letters indicate regions of qualitatively different types of shading and shadows due to a point light source.

glossiness. Leonardo's ideas about the nature of light have been fully understood and rediscovered only long after his time.

M. Faraday was the first to suggest that light should be considered as a field ('Thoughts on Ray Vibrations', 1846) much like the magnetic field. However these ideas did not receive much attention of scientists for a long time. The beginning of the era of electricity and incandescent light brought the possibility to manipulate the light flexibly and various engineering applications emerged. The typical problems engineers faced were to calculate the amount of light incident on surfaces and to design lighting setups which provide the most efficient illumination of the scenes. Those problems could be solved without sophisticated formal theory. The first systematical physical theory of the light field was developed by Gershun in 1936. He defined new physical objects representing the light field and introduced a novel terminology. Gershun's work was driven by applications in illumination engineering. He was mostly interested in deriving illumination patterns due to light sources of various shapes. The light field according to Gershun is a 5-dimensional function that describes the light traveling in every direction through any point in space which is the definition that I use through the entire thesis. In modern terminology it is essentially the radiance arriving at the point (x, y, z) from all directions (ϑ, φ).

Knowledge of the light field is important for various applications, however for a long

period of time Gershun's theory was sufficient for most applications and consequently was not improved much. With the advent of computer graphics and computer vision the subject of the light field gained a lot of attention again. Recent achievements in the area of digital photography allow to measure light fields precisely by recording all rays passing through the scene photographically. In the computer vision community the light field is known as *Lumigraph* which is essentially the collection of all light rays passing through the scene. These measurements may be used for instance for rendering tasks in computer graphics. Image based rendering allows to render an artificial object indistinguishably from a real one, which is mostly because correct illumination is used in the process of rendering. The recorded light fields may be used not only for virtual applications but also for real illuminations in a studio. For instance a face of an actor may be illuminated due to recorded light such that the quality of shadows matches with the appearance of the scene where the light was recorded.

A better understanding of the light field is also needed for applications in illumination engineering. In the field of illumination engineering the light field is studied with respect to the visual appearance of the scene. The quality of light is estimated from various parameters such as the illumination on horizontal surfaces, the cylindrical illumination, the scale of light, etc (which are frequently difficult to interpret). Typically only the light incident on the surfaces is considered to be important and the light field in 3D space ignored. These conventional light measuring techniques fail to describe the quality of illumination in its form-revealing sense and therefore new methods to measure and describe the illumination are needed.

In this thesis I consider the light field as a stationary, quasy-monochromatic Plenoptic function and study its structure by means of spherical harmonics decomposition. The measurements are performed by means of a custom made device named 'Plenopter' which is capable to measure basic low order properties of light fields in empty 3D spaces.

1.2 Overview

The main goal of this thesis is to improve existing theories of the light field by means of theoretical and empirical analysis. We address the subject of the quality of light and try to bridge the gap between scientific and artistic understandings of this concept by introducing physical parameters which describe form-revealing characteristics of light and at the same time have very intuitive interpretations which lead directly to an understanding

of object appearance. One of the main subjects in the thesis will be the global structure of the light field and its relation to the structure of the scene. We are mostly interested in the low order properties of the light field and study them both theoretically and via measurements in natural scenes. We also introduce a new measuring device capable of such measurements and describe a technique with which the low order components may be calculated for the entire scene. The core part of the thesis consists of four chapters which are independent papers and presented as they will appear in scientific journals.

In chapter 2 we study the spatial distribution of low order properties of light field in several types of natural scenes. On the basis of measurements which were done by means of a panoramic imaging technique we showed that the low order components of the light field remain practically constant along a scene as long as the geometry of the scene is fixed and the light sources remain similar. In that chapter we also address the subject of the quality of light and present an intuitive and easy interpretation of the structure of the local light field up to the second order in terms of spherical harmonics.

In chapter 3 we further pursue the empirical investigation of the structure of the light field in natural scenes conducting measurements across the axes of symmetry of the scenes such that the geometries vary from point to point. We show that the low order components of light behave similarly over scenes of similar geometries which demonstrates that the light field may be considered as a property of the geometry and material composition of the scene. This fact may be useful for modeling in computer graphics. In this chapter we present our custom made measurement device the 'Plenopter' which is capable of measuring the light field up the second order spherical harmonics approximation.

In the fourth chapter we describe a technique to recover the second order light field for the entire three-dimensional scene on the basis of discrete measurements. We also present a new way of visualizing the light field by means of light tubes, which were originally introduced by Gershun.

The fifth chapter is mostly theoretical and devoted to the possible topological structures of light fields. We provide models which show that basically all generic topological structures which occur in two-dimensional vector fields may also occur in light fields. For instance, we show a model which demonstrates that flux lines may even be closed.

In the Appendix we give additional examples which illustrate the usefulness of the results presented in this thesis and also describe methods which have not been shown in previous chapters.

In the Summary the main results of the thesis are summarized.

CHAPTER 2

LIGHT FIELD CONSTANCY

WITHIN NATURAL SCENES

Abstract

The structure of light fields of natural scenes is highly complex due to high frequencies in the radiance distribution function. However it is the low order properties of light that determine the appearance of common matte materials. We describe the local light field in terms of spherical harmonics and analyze the qualitative properties and physical meaning of the low order components. We take a first step in the further development of Gershun's classical work on the light field by extending his description beyond the three-dimentional vector field, towards a more complete description of the illumination using tensors. We show that the three first components, namely the monopole (density of light), the dipole (light vector) and the quadrupole (squash tensor) suffice to describe a wide range of qualitatively different light fields.

In the article we address a related issue, namely the spatial properties of light fields within natural scenes. We want to find out to what extent local light fields change from point to point and how different orders behave. We found experimentally that the low order components of the light field are rather constant over the scenes whereas high order components are not. Using very simple models, we found a strong relation between the low order components and the geometrical layouts of the scenes.

2.1   Introduction

Photographers, painters, designers and architects acknowledge that the quality of the light in scenes is one of the main determinants for the visual appearance of these scenes.[1, 2, 3, 4] In order to make materials look convincing one should use 'natural complex light fields' in the rendering process [5]. However, few studies [6, 7] describe the fundamental regularities of natural light fields empirically. The meaning of the term 'quality of light' and its properties in natural scenes remain unclear.

The purpose of our work is to investigate the optical properties of natural scenes. More specifically, our aim is to describe theoretically the quality of the illumination, which is a rather artistic concept, in terms of physical measures. Furthermore, we experimentally analyze the spatial properties of light fields within natural scenes. There is no common language to describe the quality of light and its effect on the appearance of an object. Different approaches are used in different fields depending on the goals. For instance, lighting engineers and designers adopt an integral approach using a wide range of parameters (luminance levels, diffuseness, uniformity, glare index and many others). On the other hand, in computer graphics the illumination is frequently simplified as much as possible; in most cases the combination of ambient and direct components does the trick. A similar approach is adopted in photographers' studios and 'movie shooting stages' where the combination of diffuse and direct light sources produces convincing results for most objects.

Light fields of natural scenes are highly complex containing low and high frequencies. Due to (inter-)reflections within scenes the light comes from every direction and therefore in general the light field cannot be determined completely solely by primary light sources. However, despite the complexity of illumination, even with the naked eye it is often possible to distinguish some basic properties of light such as the overall brightness, the primary illumination direction and the diffuseness.

The first part of the article is devoted to a theoretical analysis of second order lighting. It is convenient to analyze the properties of light fields using spherical harmonics decompositions because this allows us to represent complex lighting as a combination of components of different orders. We investigate the qualitative properties of the first three components (monopole, dipole and quadrupole) and describe their physical meanings through the development of a theoretical framework in which Gershun's classical work on the radiometric properties of the light field is related to, and extended by these

current techniques. We also develop a graphical representation of the low orders that gives a simple and intuitive description of the radiance distribution.

Another goal of our study is to investigate the dependency of the light field on the geometrical layout of the scenes. A particular question that we are addressing here is how much the illumination varies from location to location within a scene and how the different orders of the light field behave as a function of location within a scene. Taking into account that natural scenes usually have few primary light sources and that most materials scatter light in a diffuse way, we hypothesized that the low order components of the illumination should be more or less constant within a scene and depend systematically on the geometrical layout of the scene. In order to test these hypotheses we empirically investigated the light field of several scenes by measuring local light fields at several points of each scene using the panoramic image technique.

2.2   Previous work

The light field is a function that describes the amount of light traveling in every direction through every point in space. The term light field and the first systematic theory on this subject were introduced by Gershun in a paper on the radiometric properties of light in 3D space [8].

At a typical point in a natural scene light comes from all directions simultaneously. Gershun's 'light field' is essentially the radiance distribution over all space and all directions. For instance, for uniformly diffuse illumination, where the radiance is the same for all directions, the radiance distribution function at a point is a sphere. For a parallel beam of light the radiance distribution function degenerates into a single direction in the direction of the beam.

Gershun's primary goal was to describe the net transfer of radiant power through space. He defined the 'radiant flux density' as the net flux that passes through any given surface element from either side. Gershun introduced the notion of 'light vector' such that the component of the light vector in the direction of the surface normal represents the net flux density. The direction of the light vector can be found directly from the radiance as the average direction, weighted by radiance, over all directions. This concept allowed Gershun to describe the light field as a classical three-dimentional vector field. Moon and Timoshenko, who translated his work, already mentioned that 'the physically important quantity is actually the illumination, which is a function of five independent variables,

not three'. The light vector defines directly the transfer of radiant power, but does not define the full radiant structure (i.e. the lighting condition). Two light vectors may be identical whereas the radiance functions that underlie them may be quite different. In our work we introduce the quadrupole or squash tensor of the light field, to complement the light vector such as to describe the radiance distribution function in more detail. This may be considered as a small step towards the development that Moon and Timoshenko were aiming for in their foreword: 'Is it not possible that a more satisfactory theory of theory of the light field could be evolved by use of modern tensor methods in a five-dimensional manifold?'.

Gershun's theory was further developed and broadened by Parry Moon in his work on the Photic Field [9]. In different areas the concept of radiance distribution has different names: in computer vision it is known as plenoptic function [10], in the realm of computer graphics it was introduced as the Lumigraph [11] or Light Field [12] and became very popular in applications for image-based modeling and rendering. Since then, several techniques of parametrizing and capturing light fields have been developed.

The analysis of light field properties in natural scenes started from the statistical analysis of intensity distributions in conventional images of natural scenes. [13, 14] Due to the limited field of view and low dynamic range of conventional images, that approach was limited. Later Dror adopted a similar approach to high dynamic range panoramic images of the scenes, so-called 'illumination maps' (one of the ways of capturing the incoming light field at a point). He performed a statistical analysis on several illumination maps which were photographed in different scenes and found some regularities in the intensity distributions in those images. The scenes were independent of each other which leaves unanswered the questions: Is there a relation between the intensity distribution in illumination maps and the geometrical envelopes of the scenes or illumination conditions of the scenes? If there is a relation how much does the light field vary within a scene?

The spherical harmonics [15, 16] representation of the light fields appeared to be useful in many applications ranging from computer graphics rendering techniques to recognition algorithms in computer vision. It was shown theoretically [17, 18] for convex Lambertian objects that the light field can be successfully replaced by its second spherical harmonics approximation without changing the objects' appearance much.

2.3   Theory

In this section we look into the low order properties of lighting. When spherical harmonics decomposition is applied the radiance distribution function at a point can be represented as a sum of its frequency components. We give a qualitative, physical description of the components up to the second order in terms of spherical harmonics. We show that the second order component, the quadrupole or squash tensor, represents specific cases of lighting such as a 'clamp' and a 'ring' of light.

2.3.1   Spherical harmonics definitions

In order to describe the structure of light fields we utilize real spherical harmonics decomposition [15]. Any spherical function $f(\vartheta, \varphi)$ can be represented as the sum of its harmonics:

$$f(\vartheta, \varphi) = \sum_{l=0}^{\infty} \sum_{m=-l}^{l} f_{lm} Y_{lm}(\vartheta, \varphi), \tag{2.1}$$

the basis functions being defined as

$$Y_{lm}(\vartheta, \varphi) = K_{lm} e^{im\varphi} P_{lm}(\cos \vartheta), \quad l \in N, \quad -l \le m \le l, \tag{2.2}$$

where P_{lm} are the associated Legendre polynomials and K_{lm} are the normalization constants

$$K_{lm} = \sqrt{\frac{(2l+1)}{4\pi} \frac{(l-m)!}{(l+m)!}}, \tag{2.3}$$

and the real value basis is defined as

$$Y_{lm}(\vartheta, \varphi) = \begin{cases} \sqrt{2} K_{lm} \cos(m\varphi) P_{lm}(\cos \vartheta), & m > 0, \\ \sqrt{2} K_{l|m|} \sin(|m|\varphi) P_{l|m|}(\cos \vartheta), & m < 0, \\ K_{l0} P_{l0}(\cos \vartheta), & m = 0. \end{cases} \tag{2.4}$$

Spherical harmonics form an orthonormal basis on the unit sphere. Coefficients f_{lm} can be calculated as

$$f_{lm} = \int_{\varphi=0}^{2\pi} \int_{\vartheta=0}^{\pi} f(\vartheta, \varphi) Y_{lm}(\vartheta, \varphi) \sin(\vartheta) \, d\vartheta d\varphi, \tag{2.5}$$

The indices obey $l \ge 0$ and $-l \le m \le l$. Thus, order l consists of $2l + 1$ basis functions. Therefore the function can be represented as a sum of its components, i.e. different orders. Any order l can be represented as a vector of corresponding coefficients
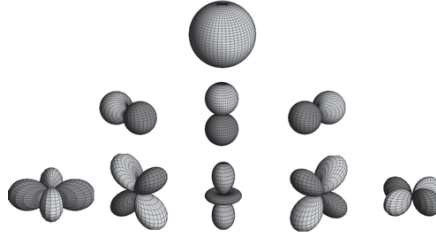
Figure 2.1: Spherical harmonics basis functions. The first row (the sphere) represents the zeros order, the second row shows the basis functions of the dipole, the third row shows the basis functions of the quadrupole.

$SH_l(f) = \{f_{l-l}, f_{l-l+1}, ..., f_{ll}\}$ and the representation of the entire function is a combination of the orders, i.e. $SH(f) = \{SH_0(f), SH_1(f), SH_2(f), ...\}$.

The spherical harmonics representation depends on the orientation of the function, i.e. if R is an arbitrary rotation over S, then $SH(f) \neq SH(R(f))$. Therefore, in general the vector of SH coefficients cannot be used as an unique descriptor of the 3D shape defined by that function. Although a rotation will change the coefficients, it does not change the energy of the orders. This property was used by Kazhdan et al. [19] to construct rotationally invariant descriptors

$$d_l = \sqrt{\sum_{m=-l}^{l} f_{lm}^2}. \tag{2.6}$$

Siegel [20] used a similar approach to characterize radiance distributions of different light sources. Physically, parameters d_l represent the power of the angular mode l. Siegel referred to d_l as the 'strength of the angular mode l'. The drawback of these coefficients is that they do not describe the function completely. For instance, if we rotated different components of a function arbitrarily and independently then the d_l profile of the resulting function would be the same, whereas the shape would be different. Therefore in general it is important to take into account the mutual orientation of different components as well as their strength.

2.3.2 Meaning of the low order components and their schematic graphical representation

For the zeroth and first order components the analogy between the spherical harmonics description and Gershun's theory is straightforward. The zero order term, the monopole $\mathbf{M} = \{f_0\}$, corresponds to Gershun's 'density of light', which is an integration of the radiance over the sphere. The monopole term is a fundamental property of the light field that describes the overall illumination at a point, i.e. how much radiance arrives at a point from all directions. From a computer graphics point of view the zero order term can be thought of as an 'ambient component'.

The first order term $\mathbf{D} = \{f_{1-1}, f_{10}, f_{11}\}$ can be thought of as a dipole, in view of the fact that in terms of spherical harmonics it consists of a positive and a negative mode. The orientation of the dipole corresponds to Gershun's 'light vector' - the direction of maximum energy transfer at the point under consideration. The concept of the light vector allows us to represent light fields as vector fields.

The second order term is the quadrupole $\mathbf{Q} = \{f_{2-2}, f_{2-1}, f_{20}, f_{21}, f_{22}\}$ which consists of five basis functions. The angular distribution according to a quadrupole is given by $Q(\vartheta, \varphi) = \sum_{m=-2}^{2} f_{2m} Y_{2m}(\vartheta, \varphi)$. Any order term with $l \geq 1$ consists of positive and negative components, and in the case of the quadrupole these components are orthogonal to each other. The orientation of the components can be found from the maximum (minimum) of $Q(\vartheta, \varphi)$. When proper rotation is applied any quadrupole can be represented as $\mathbf{Q}^{rot} = \{0, 0, q^+, 0, q^-\}$ by aligning the axes of the quadrupole along the coordinate axes - positive component along Z and the negative along Y (see Figure 2.2). This rotation provides the simplest representation of the quadrupole - just two parameters q^+ and q^- are enough to describe its shape (in other words: the quality).

Thus, the second order approximation of the radiance distribution function can be determined by a small set of meaningful parameters: the density of light d_0; the direction of the light vector (ϑ_D, φ_D) and its strength d_1; the orientations of the quadrupole's axes $(\vartheta_{Q+}, \varphi_{Q+})$ and $(\vartheta_{Q-}, \varphi_{Q-})$ and parameters q^+ and q^-. See Figure 2.3(a) for a schematic representation in which the arrows indicate the orientations of the light vector and axes of the quadrupole, and the lengths of the arrows are proportional to their strength: the values of d_1, q^+, q^-. This graphic representation together with the value d_0 completely determines the second order lighting. Parameters d_0, d_1, d_2, q^+ and q^- can be used as a rotationally independent characterization of the light field.

The second order representation can be further simplified by rotating the function in

		0.282		
	0.064	0.216	-0.064	
0.029	0.072	0.019	0.002	0.044

(a)

		0.282		
	0.149	0.181	0.007	
0	0	0.093	0	-0.020

(b)
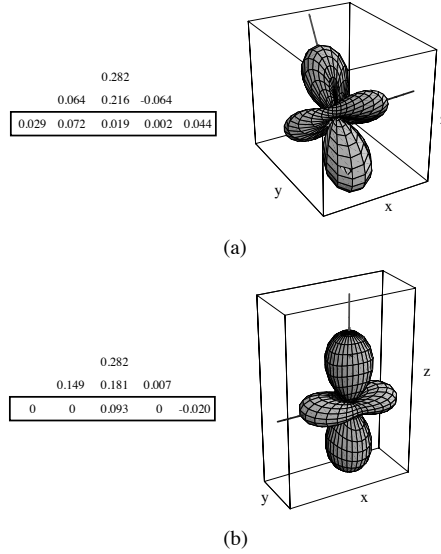
Figure 2.2: Second order representation of a light field in the (a) original arbitrary orientation and (b) orientation with regard to the quadrupole. On the left side the first nine coefficients are presented (note the change after rotation); on the right side the quadrupoles are presented graphically. Note that the shape of the quadrupole does not change after rotation whereas the mathematical description is simplified and depends only on two coefficients $q^+ = 0.093$ and $q^- = -0.020$. The coefficients that make up the quadrupole are framed.

such a way that the components are aligned according to the coordinate's frame. Since the dipole is the strongest component in most cases (except for the monopole, which does not have an orientation), it might be more convenient to orient the light field according to the dipole such that the light vector is parallel to Z. Then the second order representation of the light field will be $SH_2^D(LF) = \{\mathbf{M}^D, \mathbf{D}^D, \mathbf{Q}^D\} = \{\{d_0\}, \{0, d_1, 0\}, \{f_{2-1}^D, f_{2-1}^D, f_{20}^D, f_{21}^D, f_{22}^D\}\}$ (see Figure 2.3(b)). A rotation does not change the structure of the radiance distribution function, but it changes its orientation in global coordinates. The mutual orientation of the dipole and quadrupole remains the same under rotation. Because the light vector is fixed, the second order description will now consist of eight parameters: $d_0, d_1, \vartheta_{Q^+}, \varphi_{Q^+}, \vartheta_{Q^-}, \varphi_{Q^-}, q^+, q^-$.

15

0.282

-0.063   0.226   -0.040

-0.018 -0.012   0.099   -0.066   0.045

(a)

0.282

| 0 | 0.225 | 0 |

0.032   -0.011   0.107   0.062   0.028

(b)

0.282

0.064   0.216   -0.064

| 0 | 0 | 0.127 | 0 | -0.038 |

(c)
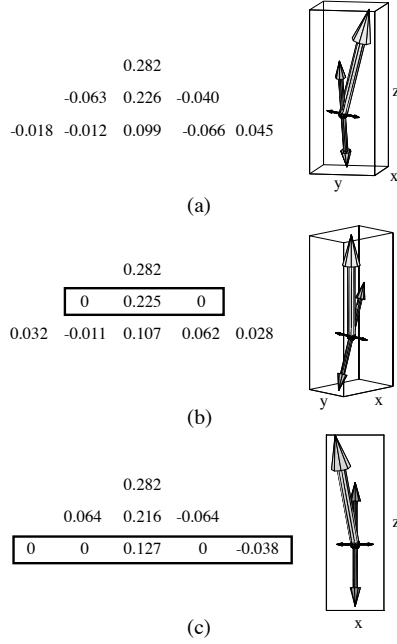
Figure 2.3: Schematic graphical representations of the second order light field in (a) the original orientation and (b) the orientation aligned according to the light vector (c) the orientation aligned according to the quadrupole. The SH coefficients are presented on the left side. The mutual orientation of the components D, $q+$ and $q-$ is shown on the right side. The length of the light gray arrow corresponds to the value d_1 (strength of the light vector), the lengths of the dark gray and black arrows correspond to values $q+$ and $q-$.

In a similar way we can rotate the function in such a way that the axes of the quadrupole, which are orthogonal to each other, are oriented according to the coordinate axes Z and Y (see Figure 2.3(c)). Then the second order lighting is given by

$$SH_2^Q(LF) = \{\mathbf{M}^Q, \mathbf{D}^Q, \mathbf{Q}^Q\} = \{\{d_0\}, \{f_{1-1}^Q, f_{10}^Q, f_{11}^Q\}, \{0, 0, q^+, 0, q^-\}\}. \qquad (2.7)$$

So here the structure of second order light field, which is independent of orientation, is given by six parameters: $d_0, d_1, \vartheta_D, \varphi_D, q^+, q^-$.

In all three cases (Figure 2.3 a, b, c) the structure of the light field is the same. The rotation only changes its orientation in the global coordinate frame, whereas the mutual

16

orientation of the components, their quality and strength are the same. The representation in Figure 2.3(a), shows the original orientation of a light field in the global coordinate frame, is useful when, for instance, we want to couple the radiance distribution function to the scene geometry. On the other hand, if we are interested only in the structure of the light field then representation (7) is more convenient because it restricts the coordinate frame and consists of fewer parameters.

The qualitative properties of the quadrupole are described in the next section.

2.3.3 Qualitative properties of the quadrupole

The quadrupole has two components: one positive and one negative, which are orthogonal to each other and symmetric around the intersection point. As was shown in the previous section, the structure (quality) of a quadrupole can be described completely by two scalar parameters q^+ and q^-. Therefore keeping the strength of the quadrupole constant (d_2 constant) and varying q^+ and q^- such that $\sqrt{(q^+)^2 + (q^-)^2} = d_2$ we can achieve all possible structures of the quadrupole. The most extreme cases of light fields due to a quadrupole alone (light vector is assumed to be zero, the monopole component chosen as small as possible such that the resulting function is nonnegative) appear to be a light clamp $q^+ = 1, q^- = 0$ and a light ring $q^+ = 0.5, q^- = \sqrt{3}/2$, see Figure 2.4.

Figure 2.4(a) physically corresponds to two equal diffuse light sources positioned opposite to each other, we call this a 'light clamp'. Figure 2.4(b) corresponds to a diffuse 'ring light source'. Roughly speaking, from the coefficients q^+ and q^- we can assess how close the quadrupole is to one of those extreme cases.

By adding a light vector and changing the strengths and mutual orientations of the three components we can achieve a wide range of topologically different light fields.

2.3.4 Models for simple geometries: Street, Wall, Forest scenes

In order to provide a more intuitive explanation of the light vector and quadrupole we will consider some very simple models of the light fields in several basic geometries. The geometrical layouts of the scenes are depicted schematically in Figure 2.5.

The model of the open field scene consists of a uniformly bright sky (upper hemisphere) and uniformly bright ground (lower hemisphere) which is darker than the sky. The second order representation of a light field in such a scene will contain only the light vector and the monopole. The quadrupole vanishes due to the symmetry of the brightness

(a)   (b)
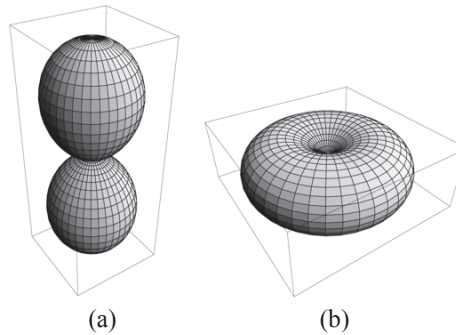
Figure 2.4: Qualitative properties of the quadrupole. Extreme cases of light fields due to the quadrupole: (a) a light clamp, $q^+ = 1, q^- = 0$, (b) a light ring, $q^+ = 0.5,\quad q^- = \sqrt{3}/2$. The light vector is assumed to be zero, the monopole d_0 is chosen as small as possible such that the resulting function is nonnegative everywhere.

distribution function in the scene (in fact, all even components vanish). The light vector is oriented vertically to the middle of the sky opening and in this case indicates the symmetry of the light field. Due to the non-uniformity of materials and geometry in natural scenes (the sky is not uniformly bright, the ground is not Lambertian, the geometrical layout is not symmetrical), the brightness distribution function cannot be absolutely symmetrical and therefore in natural scenes the quadrupole generally does not vanish completely. However, in the scenes which are close to our assumptions (heavily overcast sky, uniform ground close to Lambertian, open space up to horizon) the quadrupole should become negligibly small in comparison with the light vector.

Figure 2.6(a) shows the model of the light field across a street scene. Again, the sky is assumed to be uniformly bright, the ground and the walls are uniform and Lambertian (the ground is brighter than the walls), interreflections were not taken into account. We calculated the local light fields in five points across the scene. The light vector tends to be oriented approximately in the direction of the middle of the sky opening (direction of maximum energy transfer) and its orientation changes gradually from location to location; $\mathbf{q}^+$ is oriented primarily vertically according to the 'clamp' composed of the brightest areas in the scene - sky and ground; $\mathbf{q}^-$ is oriented according to the darkest areas in the scene (walls), which can be thought of as a negative clamp. Note that the orientation of light field components changes smoothly as the geometrical layout changes.
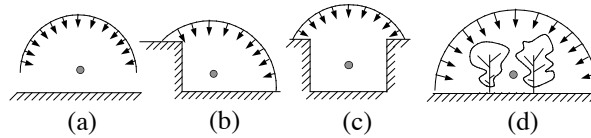
Figure 2.5: Geometrical layouts of the measured scenes (a) open field (b) wall (c) street (d) forest.

Figure 2.6(b) depicts the wall scene, which is essentially the same as the street scene but without one wall. Note that the strength of the quadrupole decreases as the distance to the wall increases and the closer the situation gets to the open field scene.

In order to investigate a scene in which the geometry varies more stochastically than in man-made scenes, we considered a forest scene. The illumination in a forest is due to the light scattering through the foliage and the gaps in the foliage. The upper hemisphere of the scene was modeled as a random distribution of $30°$ patches each of different brightness. The lower hemisphere was modeled in the same way but the mean brightness value was lowered. We calculated the local light fields at three points of this scene. The results are shown in Figure 2.6(c); the orientation of the light vector is vertical and varies a little from location to location, whereas the orientation of the quadrupole is random.

It was not our purpose to develop sophisticated detailed models of natural scenes; on the contrary, we tried to simplify them as much as possible. However, as it will be shown in the section on empirical studies, the light fields of corresponding real natural scenes show similar patterns to those of our much oversimplified models.

2.4 Empirical studies

In the empirical study we considered three types of scenes, namely a city street, a forest and a wall (see Figure 2.5). These scenes were chosen because they are common, simple (also to model), and possess different properties: the street and wall scenes have very distinct geometries; the geometry of the forest scene, on the other hand, is rather stochastic and does not have a clear envelope. Each type of scene was measured under two types of natural daylight illumination conditions: clear sky (close to collimated) and overcast sky (rather diffuse).
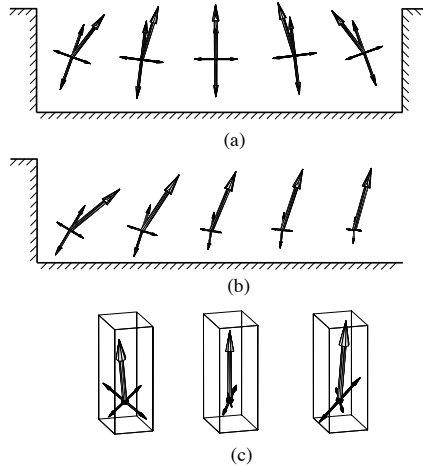
Figure 2.6: The simplest models of light field in the following geometries a) street scene (b) wall scene (c) forest scene.

2.4.1 Data acquisition

In order to estimate how the light field changes within each scene, we took three samples per scene at different locations. The samples were taken along a straight line, approximately 10 meters apart and at a height of 1.5 meters. The orientation of the line, along which the measurements were taken, was chosen in such a way that the geometrical layout of a scene remained approximately the same as viewed from the measurement locations. In the case of the city-street scene the measurements were taken along the street; for the forest the direction of measurements was not important due to the isotropic character of the geometry of that scene (though of course it was kept constant with relation to the primary illumination). The 'wall' scene was measured in two directions: along the wall, such that the geometry remained the same, and across the scene, orthogonally to the wall such that the geometrical layout varied systematically with distance.

At every point the local light field was measured as an illumination map: a high dynamic range panoramic image covering a whole sphere. To produce the panoramic image we used an Olympus E-20 digital camera with a fish-eye lens, attached to a rotation frame and mounted on a leveled tripod. We used a fish-eye lens with a 124° horizontal field of view. Each panorama consisted of 14 images made in different directions (the

20

pictures overlapped by 30% to achieve a better result). In order to increase the dynamic range the pictures were taken with three different exposure values. The pixel-by-pixel correspondence between the pictures of different exposures was achieved by using remote control and by making the pictures in the automatic bracketing mode.

The whole procedure of taking the pictures for three panoramas (126 pictures) took about 40 minutes. The time for making measurements was chosen around noon, so that the sun did not move much during measurements and therefore illumination was relatively constant.

2.4.2   Data processing

The images were corrected for radial brightness fall-off and stitched together in a rect-angular panoramic image. For this purpose we used commercially available software PTMac 3.00. The stitching procedure was applied separately for different exposures and three resulting panoramas were combined together into one high dynamic range illumi-nation map according to the radiance response curve of the camera. The response curve was estimated using a technique described by Debevec and Malik [21]. The high dy-namic range pictures were stored as arrays of floating-point values. The resolution was downsampled to 250×500.

2.5   Results

The panoramic images of the scenes considered are shown in Figure 2.7 in a light probe format [22] (angular map). For each image we calculated spherical harmonic coefficients up to the 6th order. To the right of the panoramic images we depicted the cross-sections through the SH_6 approximations of the corresponding local light fields, the directions of the cross-sections being indicated by black circles in the panoramic images. The panoramic images show the actual scenes, whereas the cross-sections give an impres-sion of how the 6th order approximation of light field varies within scenes. For instance, in the panoramic images of the street scene under clear sky illumination condition (Fig-ure 2.7(a)) there are two bright areas due to the sun (top right; note: the sun itself is not present in either of the panoramas) and due to strong scattering from the building on the left side of the street. These two brightest areas are distinguishable in the cross-sections as modes in the corresponding directions. Note that the mode that corresponds to the
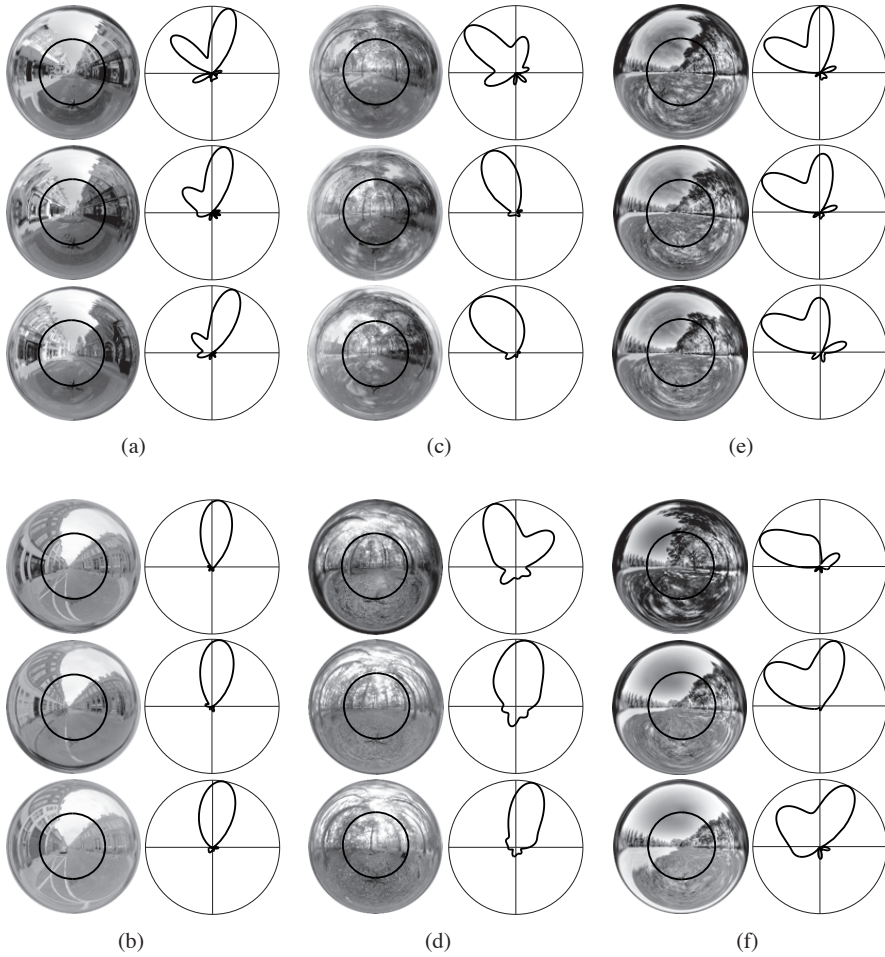
Figure 2.7: The light probes of (a) a street scene under a clear sky, (b) a street scene under an overcast sky, (c) a forest under clear sky (d) a forest under an overcast sky (e) a 'wall' scene measured along the wall (f) a wall measured across. Tho the right of the panoramic images the cross-sections through the SH_6 approximations of the corresponding local light fields are depicted; the directions of the cross-sections are indicated by black circles in the panoramic images.

bright sky area is stronger and the same in all three locations, whereas the second mode is hardly distinguishable in the third location (this is because the cross-section line runs through the relatively dark spot on the left building).

A similar situation exists in the 'wall along' scene (Figure 2.7(e)) in which one mode is due to the large opening in the sky on the left side of panoramas, and the second one is due to bright halo around the sun (the sun is hidden behind the trees). Note how similar the profiles are for all three locations of this scene. In the 'wall across' scene the geometrical layout of the scene varies from location to location and you can see (Figure 2.7(f)) how the cross-sections of the light fields transform from one mode at the first location into two modes at the third location.

In the forest scenes (Figures 2.7(c,d)) the primary sources of light are patches of open sky from the gaps in the foliage which are distributed rather stochastically over the upper hemisphere [23]. Therefore the radiance distribution function varies considerably. However, from the cross-sections we can see that for each location there is only one strong mode which is oriented approximately vertically (light comes from above) but is slanted slightly in the direction of the largest opening in the foliage.

Note that because the panoramic images were photographed in equal orientations at all three measurement points of each scene, we can use the spherical harmonics coefficients and the cross-section profiles (which are calculated from spherical harmonics coefficients) to compare the local light fields straightaway without a having to calculate the rotationally independent parameters.

Figure 2.8 shows the schematic representation of the second order approximation of the samples. As was explained in section 3, this kind of representation gives the complete description of the second order approximation of the local light fields. Comparing different samples you can see how the light vector changes its orientation and magnitude, how the quality and orientation of the quadrupole change from point to point. This kind of representation enables us to judge qualitatively the behavior of the low order components of the light fields. The spherical harmonic coefficients for each sample were normalized by the zero order component in order to give equal footing comparisons (here we are mainly interested in the structure of light fields, not in the absolute values).

In Figure 2.9 we depict the strengths of the different orders, i.e. coefficients d_l up to the 10th order. The parameter d_0 is equal to 1 for all samples in all scenes, because the spherical harmonics coefficients were normalized by the zero order component. Coefficients d_l provide rotationally independent descriptors and physically represent the power
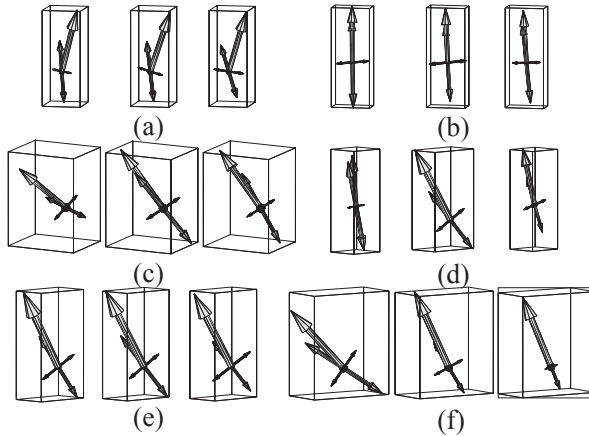
Figure 2.8: A schematic representation of the second order approximations of the local light field measurements. The letters represent the same scenes as in Fgure 7.

of the corresponding angular mode l. Note that strengths of low orders are higher than those of high orders. Starting from the 4th to 5th order the d_l values fade away and level off at a value which is significantly smaller (approximately 5 times smaller) than the strengths of low orders.

2.6 Conclusion and discussion

From Figures 2.7 and 2.8 we can conclude that in the case of overcast diffuse illumination the light field varies less than in the case of clear sky. That is easy to explain from the properties of the scenes considered. As we can see from the panoramic images, in the 'street' scenes the primary illuminations and geometrical layouts of the scenes are reasonably constant in the locations where the samples were made. Light field variation is mainly due to the secondary light sources, which vary within a scene due to the variation of the reflectance properties of materials that make up the scene, from location to location in that scene. The effect of these secondary light sources is much stronger in collimated illumination (clear sky) than in diffuse lighting (overcast sky) due to the directedness of the primary illumination. In the case of 'forest' scenes, the light field variation is due to two factors - the geometrical layout of the scenes varies (the gaps in the foliage
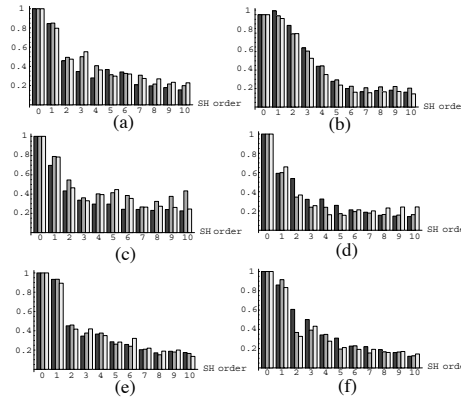
Figure 2.9: The strengths d_l of the light field components up to 10th order. The letters represent the same scenes as in Figure 7; the bars of different gray levels represent three samples within scene.

are stochastic) and secondary light sources are more significant in the case of clear sky illumination (note bright patches on the ground in the scene 'c').

From Figures 2.7 and 2.8 we can also say that the low order components of light field are more constant within a scene than are the high orders. Note in Figure 2.8 that as long as the geometry of a scene remains reasonably constant, the low orders are very similar in different locations. However, if the position with regard to the geometry varies systematically, the low order components vary systematically as well. The simple model of the wall scene (Figure 2.6(b)) corresponds well to real measurements (Figure 2.8(f)); notice a similar tendency in component orientations and observe how the quadrupole decreases as the distance to the wall increases.

Figure 2.9 shows that the low order components of the light fields within the scenes considered are the strongest. Low order components define the main shape of the light field, whereas the higher orders have a more stochastic nature. We believe this fact can be used in modeling - the main properties of the light field (shape of the radiance distribution function) can be defined by low orders (density of light, light vector, quadrupole), whereas the high orders can be taken as stochastic values that do not change the main properties of the light field, but add naturalness to it.

BIBLIOGRAPHY

[1] A. Adams, *The negative* (Little, Brown and Company, 1981).

[2] T. S. Jacobs, *Drawing with an Open Mind* (Watson-Guptill, 1991)

[3] L. Michel, *Light: the space of shape* (John Wiley, 1995).

[4] M. Baxandall, *Shadows and enlightenment* (Yale University Press, 1995).

[5] R. W. Fleming, R.O. Dror, E. H. Adelson, 'Real-world illumination and the perception of surface reflectance properties,' J. Vision **3**, 347-368 (2003).

[6] R.O. Dror, T.K. Leung, E.H. Adelson, and A.S. Willsky, 'Statistics of Real-World Illumination,' in *Proceedings of the IEEE Computer Society Conference on Computer Vision and Pattern Recognition*, (IEEE, 2001), pp. 164-171.

[7] R.O. Dror, A.S. Willsky, E.H. Adelson, 'Statistical characterization of real-world illumination,' Journal of Vision **4**, 821-837, (2004).

[8] A. Gershun, 'The light field,' J. Math. Phys. 18, 51151. (1939) (translated by P. Moon and G. Timoshenko).

[9] P. Moon, D. E. Spencer, *The Photic Field*, (MIT Press, 1981).

[10] E. H. Adelson and J. Bergen, 'The plenoptic function and the elements of early vision,' in *Computational Models of Visual Processing*, M. Landy, and J. Movshon, eds. (MIT Press, 1991), pp. 3-20.

[11] S. J. Gortler, R. Grzeszczuk, R. Szeliski, and M. F. Cohen, 'The lumigraph,' in *Computer Graphics, Proc. SIGGRAPH96*, (1996), pp. 43-54.

[12] M. Levoy and P. Hanrahan, 'Light field rendering,' in *Proc. SIGGRAPH 96*, (1996), pp. 31-42.

[13] J. Huang, D. Mumford, 'Statistics of Natural Images and Models,' in *Computer Vision and Pattern Recognition* (IEEE, 1999), pp. 541-547

[14] S. Teller, M. Antone, M. Bosse, S. Coorg, M. Jethwa, and N. Master, 'Calibrated, registered images of an extended urban area,' in *Proc. IEEE Computer Vision and Pattern Recognition* (CVPR, 2001), pp. 93-107.

[15] T. MacRobert, *Spherical harmonics: an elementary treatise on harmonic functions, with applications* (Dover Publications, 1947).

[16] J. Jacson, *Classical Electrodynamics* (John Wiley, 1975).

[17] R. Ramamoorthi, and P. Hanrahan, 'On the relationship between radiance and irradiance: determining the illumination from images of a convex Lambertian object,' J. Opt. Soc. Am. A. **18(10)**, 2448-2459(2001).

[18] P.N. Belhumeur, and D.J. Kriegman, 'What Is the Set of Images of an Object under All Possible Illumination Conditions?' Int'l J. Computer Vision **28**, pp. 245-260 (1998).

[19] M. Kazhdan, T. Funkhouser, and S. Rusinkiewicz, 'Rotation Invariant Spherical Harmonic Representation of 3D Shape Descriptors,' in *Eurographics Symposium on Geometry Processing*, L. Kobbelt, P. Schrder, H. Hoppe, ed. (EG Digital Library, 2003).

[20] R. D. Stock and M. W. Siegel, 'Orientation Invariant Light Source Parameters,' J. Opt. Eng. **35**, pp. 2651-2660 (1996).

[21] P.E. Debevec and J. Malik, 'Recovering high dynamic range radiance maps from photographs,' in *Proceedings of ACM SIGGRAPH* (1997), Annual Conference Series pages 369-78, 1997

[22] http://www.debevec.org/Probes/

[23] J. A. Endler, 'The color of light in forests and its implications,' in *Ecological Monographs 63* (Ecological Society of America, 1993), pp.1-27.

CHAPTER 3

THE STRUCTURE OF LIGHT FIELDS IN NATURAL SCENES

Abstract

Light fields [1, 2] of natural scenes are highly complex and vary within a scene from point to point. However, in many applications complex lighting can be successfully replaced by its low order approximation [3, 4]. The purpose of this research is to investigate the structure of light fields in natural scenes. We describe the structure of light fields in terms of spherical harmonics and analyze their spatial variation and qualitative properties over scenes.

We consider several types of natural scene geometries. Empirically and via modeling we study the typical behavior of the first and second order approximation of the local light field in those scenes. The first order term is generally known as the 'light vector' and has an immediate physical meaning. The quadrupole component which we named 'squash tensor' is a useful addition as we show in this paper. The measurements were done with a custom-made device of novel design, called 'Plenopter', that was constructed for measuring the light field in terms of spherical harmonics up to the second order.

In different scenes of similar geometries we found structurally similar light fields, which suggests that in some way the light field can be thought of as a property of the geometry. Furthermore, the smooth variation of the light field's low order components suggests that instead of specifying the complete light field of the scene it is often sufficient to measure the light field only in a few points and rely on interpolation to recover the light field at arbitrary points of the scene.

3.1   Introduction

The quality of the light field, i.e. the directional properties of the illumination, strongly affects the appearance of an object positioned at that point [5, 6, 7, 8, 9, 10]. For instance, in fully diffuse illumination even a specular metallic object looks rather matte. Diffuse illumination can very well have directional properties, for instance, the illumination from an overcast sky is directed vertically downwards. However, the properties of diffuse and highly directional (collimated) illumination are very different. In collimated illumination the shading is dominated by the presence of body and cast shadows, whereas in diffuse illumination shading gradients are much more gradual and much of the shading is actually due to vignetting. The surface structure of rough surfaces gives rise to texture in the case of collimated illumination, whereas it is hardly evident in the case of diffuse illumination. The light fields of natural scenes are often highly complicated functions, in general the angular variations can be almost arbitrary, ranging from smooth (such as under an overcast sky) to very spiky (such as on a sunny day on the beach or the light patches in a forest) [11, 12, 13, 14, 15].

Because surface elements of a convex object are illuminated from half spaces, the surface irradiance is typically fairly smooth, even if the angular distribution of the radiance is spiky [5, 6]. If the primary and secondary light sources are relatively distant from the region of interest, the spatial variations of the angular distribution will be minor over that region. Indeed, we have shown that although high order properties of the light field vary rapidly over the scene (due to specularities, albedo variations and so on), the low order properties of the light field (ambient light, degree of diffuseness, primary direction of light, or what some artists call the 'quality of light') stay rather constant as long as the geometry of the scene does not change much [4].

Gershun has introduced the very useful and intuitive notion of 'light field' [1]. The light field is just the radiance as a function of location and direction. In computer graphics it is known as the plenoptic function [16]. At any point in space the light field is a function of direction (spherical function). The radiance can be an almost arbitrary function of location and direction. Of course, it is non-negative throughout. Another constraint is that in empty space the radiance in a certain direction does not change as one moves in that direction. In this paper we are primarily interested in the illumination of diffusely scattering surfaces. The implication is that only the low-pass structure of the radiance is of importance[3]. This suggests that the Fourier description might be useful. For a

spherical function such as the light field this comes down to spherical harmonics. A simple demonstration shows that the low orders of light fields in natural scenes change rather smoothly and systematically over the scene: if we take a matte convex object and move it around the scene its appearance changes very slowly except for points which are close to large objects (like a wall) or that occlude a large part of the primary illumination. In this article we address the question of how the structure of the light field varies over the scene and what is the relation between the scene geometry and the quality of light in that scene.

We analyze the structure of light fields in terms of spherical harmonics and consider the structural properties up to the second order. It has been shown that this allows sufficiently accurate quantitative description of the shading of Lambertian surfaces[3]. For heuristic purposes it is useful to consider the qualitative structure of the zeroth, first and second order terms in the spherical harmonic development individually. The spherical harmonic development is usually known as a multipole development in physical context. The zeroth order is represented by the monopole (a scalar) and describes the 'ambient light' of computer graphics. The first order is represented by the dipole contribution. The dipole transforms as a vector, it is the light vector as defined by Gershun. The light vector describes the transportation of radiant energy through surface elements. The second order describes the quadrupole contribution. Gershun does not explicitly discuss this order of approximation. The translators of Gershun's classical paper, Moon and Timoshenko, already mentioned 'The light field considered in this book is a classical three-dimensional vector field. But the physically important quantity is actually the illumination, which is a function of five independent variables, not three. Is it not possible that a more satisfactory theory of the light field could be evolved by use of modern tensor methods in a five-dimensional manifold? We must look to the mathematician for any such development'. In this paper we develop an intuitive notion of the quadrupole field as the 'squash tensor'.

The monopole contribution describes a constant illumination from all directions. This is usually known as ambient illumination in computer graphics [17], or Ganzfeld illumination in psychology [18]. Formally, the monopole contribution at a given point is simply the average radiance over all directions. From a physical perspective, it describes the local volume density of radiation, measured in terms of photon density or total ray length per unit volume. An operational definition simply uses a spherical photocell or a translucent spherical shell with a photosensor in its interior [1]. Light fields in which the monopole

contribution dominates are rare in nature. An example is an overcast sky over a snow cover, giving rise to 'polar white-out'.

The dipole contribution describes a unidirectional light field. Because the radiance is non-negative, pure dipole fields cannot be implemented. The combination of a monopole and a dipole term yields what is known as the 'point source at infinity with ambient term' of computer graphics [17]. Formally, the light vector describes the net transport of radiant power [1]. Thus, the transport of radiant power can be visualized by way of the field lines of the 'light vector'. These field lines do not coincide with the light rays, for instance, they can be curved and even closed. In empty space, the light field has zero divergence. The light vector can be measured by way of a back-to-back sandwich of two planar photocells. Their difference signal yields the component of the light vector in the direction of the surface normal. A natural light field that approximates a dipole dominated light field is the overcast sky. A simple approximation that is often useful is the hemispherical diffuse source.

The quadrupole contribution transforms as a symmetric traceless tensor. An operational definition similar to the photocell sandwich suggested by Gershun for the dipole component can be based on a cube with flat photocells as faces. In order to measure the quadrupole one has to search for the canonical orientation (see below). A simpler way to measure the quadrupole tensor involves radiance measurements for a larger number of directions. In that case the instrument can be used in any orientation. We describe such a instrument in this paper. Quadrupole dominated light fields occur in the case of ring sources or two point sources at opposite sides of the region of interest [19, 20]. We refer to the quadrupole field as the squash tensor [4], which describes the geometry of these configurations.

The light field at a certain location in a scene depends both on the location, magnitude and directional properties of the primary light sources and on the geometry and scattering properties of the environment (for examples see Figure 3.1). The influence of the geometry is two-fold. One important effect is the obstruction of the primary illumination. In highly directional light fields one speaks of body and cast shadows, in more general cases, in which sources can be partially occluded, the effect is known as vignetting. The other effect is due to multiple scattering between different, even remote, parts of the scene. This effect is sometimes known as 'interreflection' or 'reflexes'. Both vignetting and interreflections depend strongly on the geometry of the scene. Since the radiation balance is described by a linear integral equation of the Fredholm type [21] the variance effects

Figure 3.1: From left to right a matte convex object under a collimated source from above on a black, absorbing ground (vertically oriented dipole) and on a white ground causing a secondary source from below (combination of vertically oriented dipole and quadrupole). Next the object was illuminated by collimated sunlight from the left plus ambient light (monopole plus almost horizontally oriented dipole) and with a white screen at the right causing a secundary source from the right (dipole plus almost horizontall oriented dipole and quadrupole).

can be decoupled. The so-called pseudo-facets depend only on the scene, not on the primary sources. In some cases the resulting light field is almost purely due to the geometry. An example of a geometry-dominated effect due to vignetting is the general low irradiance of surfaces inside concavities, for instance the eye sockets in a face illuminated by an overcast sky are usually dark. An example of a geometry-dominated effect due to interreflection is the integrating sphere. The light field in the interior will be monopole-dominated irrespective of the primary sources. The contribution of the reflected light to the global light field is usually less significant than the primary illumination (due to the fact that albedo in natural scenes is rather low, and besides, the materials in natural scenes are mostly matte, therefore the reflected light is rather diffuse), but still yield a noticeable effect.

The global layouts of the scenes can vary a lot depending on the environment. A generic example is an open landscape, which is also the simplest one - the light field consists of the primary illumination which is coming from the upper hemisphere and constant everywhere over the scene (due to the absence of objects that may occlude the primary light) and a diffuse reflected beam from the ground which can vary over the scene due to albedo variation. The light field in such a scene is almost constant everywhere. A

more complex type is the forest scene - here the primary illumination is due to the light that comes through openings in the foliage and therefore the local light fields are very 'spiky'. The high orders vary a lot over such a scene, however the low order properties are rather stable (these properties of course depend on the weather condition and the density of the foliage) - the dominant illumination direction is primarily from above, and the ambient component does not change much either. Urban scenes in general are more structured. However one can distinguish certain patterns of geometrical layouts which are very typical, for instance a 'wall', 'street' and, for indoor scenes, 'room' profiles. In these cases the primary illumination is due to the visible part of sky, which varies very systematically with the location in the scene. The regularity in geometry suggests that the low order components of the light field would vary in a systematic manner as well. The reflective properties of materials present in the scene define scattering and interreflections. The exact angular distributions of the material reflectances are less important (though the albedos are). Taking into account the major role of scene geometry and smooth variation of the low orders we expect that in scenes of similar geometrical layouts one should expect to find qualitatively similar low order light fields. In that sense the light field can be thought of as a property of the geometry.

In order to test our hypothesis we measured low order components (light density, light vector and the squash tensor) of light fields in natural scenes. We considered simple and frequently found in nature 'street', 'wall' and 'room' geometries in different illumination conditions. We also developed simple models of these scenes and found a strong correspondence between real measurements and our simplified models.

For measurements we used a custom made device which we named 'Plenopter' which is designed to measure light fields up to the second order in terms of spherical harmonics. Up to our knowledge the light measuring devices currently available on the market are capable of measuring the structure of local light fields only up to the first order. Measuring light fields up to the second order is a useful addition in the analysis of the structure of light fields, because the squash tensor is a significant characteristic of natural light fields. Therefore we believe that our measurement device forms a major innovation in this field. Additional to the main goal of this investigation we summarize the technical details of the design of our measurement system.

3.2 Theory

The concept of 'the light field' was introduced by Gershun in the nineteenthirtees. Gershun considers the scalar field of radiation volume density and the vector field of net flux propagation. Gershun's 'light vector' $\mathbf{D}$ is defined such that for any oriented surface element dA the net flux $d\Phi = \mathbf{D} \cdot dA$ where the sign indicates the direction of net flux propagation. The formal properties of Gershun's light field were further developed by Moon and Spencer. In this paper we extend the formalism to include second order properties of the light field.

The light field is defined by Gershun as essentially a low order approximation to the radiance. The radiance is a function of position and direction that completely describes the luminous environment. Gershun's scalar field is the zeroth order and Gershun's vector field the first order approximation to the radiance. This is essentially the initial part of a development of the radiance in terms of spherical harmonics.

3.2.1 Second order properties of the light field

The local light field at a fixed point in space is a spherical function (radiance as a function of direction) $f(\vartheta, \varphi)$ and can be represented as the sum of its harmonics:

$$f(\vartheta, \varphi) = \sum_{l=0}^{\infty} \sum_{m=-l}^{l} f_{lm} Y_{lm}(\vartheta, \varphi), \tag{3.1}$$

the real valued basis functions are defined as

$$Y_{lm}(\vartheta, \varphi) = \begin{cases} \sqrt{2} K_{lm} \cos(m\varphi) P_{lm}(\cos\vartheta), & m > 0, \\ \sqrt{2} K_{l-m} \sin(-m\varphi) P_{l-m}(\cos\vartheta), & m < 0, \\ K_{l0} P_{l0}(\cos\vartheta), & m = 0. \end{cases} \tag{3.2}$$

where the P_{lm} are the associated Legendre polynomials and K_{lm} are normalization factors

Spherical harmonics form an orthonormal basis on the unit sphere. Coefficients f_{lm} can be calculated as

$$f_{lm} = \int_{\varphi=0}^{2\pi} \int_{\vartheta=0}^{\pi} f(\vartheta, \varphi) Y_{lm}(\vartheta, \varphi) \sin(\vartheta) \, d\vartheta \, d\varphi, \tag{3.3}$$

One has $l \geq 0$ and $-l \leq m \leq l$. Thus, order l consists of $2l + 1$ basis functions. In the rotations of the coordinate system the coefficients transform for each order individually,

that is to say, the orders don't 'mix'. Therefore the radiance can be represented as a sum of its components of different orders. The zeroth order represents Gershun's scalar field and the first order Gershun's vector field. Any order l can be represented as a list of corresponding coefficients $SH_l(f) = \{f_{l-l}, f_{l-l+1}, ..., f_{ll}\}$ and the representation of the entire function is a combination of the orders, i.e. $SH(f) = \{SH_0(f), SH_1(f), SH_2(f), ...\}$.

The *monopole* component, that is the zeroth order term $\mathbf{M} = \{2\sqrt{\pi}f_0\}$, corresponds to Gershun's 'density of light' or 'space illumination'. It is essentially the average radiance. The monopole term is a fundamental property of the light field that describes the overall illumination at a point, i.e. how much radiance arrives at a point from all directions. From a computer graphics point of view the zero order term can be thought of as an 'ambient component'.

The *dipole* component, that is the first order term $\mathbf{D} = \{f_{1-1}, f_{10}, f_{11}\}$ transforms as a vector. This vector corresponds to Gershun's 'light vector' - the direction of maximum energy transfer at the point under consideration. The projection of the light vector on any direction results in flux density in that direction. Rotating the dipole in such a way that it is aligned with the z-axis it can be represented as $\mathbf{D}^{rot_d} = \{0, 0, v\}$, where $v = 2\sqrt{\frac{\pi}{3}}\sqrt{f_{1-1}^2 + f_{10}^2 + f_{11}^2}$ is the magnitude of the light vector. From a computer graphics point of view the first order term can be thought of as a diffuse directional beam.

The *quadrupole* component, that is the second order term $\mathbf{Q} = \{f_{2-2}, f_{2-1}, f_{20}, f_{21}, f_{22}\}$ consists of five basis functions. Under rotations these components transform as a symmetric tensor of trace zero. We refer to it as the 'squash tensor'. By a suitable rotation any quadrupole can be represented as $\mathbf{Q}^{rot_q} = \{0, 0, q^+, 0, q^-\}$. The two coefficients q^+ and q^- represent basis functions f_{20} and f_{22} and completely describe the structure (quality) of the squash tensor.

By a suitable rotation of the axis, the spherical harmonic development can be reduced to a convenient canonical form. We consider two possibilities. In case the dipole dominates the squash tensor (the generic case) a convenient canonical form is

$$SH_2^{rot_d}(LF) = \{\mathbf{M}^d, \mathbf{D}^d, \mathbf{Q}^d\} = \{\{d_0\}, \{0, 0, v\}, \{f_{2-2}^d, f_{2-1}^d, f_{20}^d, f_{21}^d, f_{22}^d\}\}. \qquad (3.4)$$

In this case we require 7 coefficients. The remaining two degrees of freedom are absorbed by the rotation of the axes. In case the squash tensor dominates the dipole (at singular points of the vector field) it is more convenient to use the canonical representation

$$SH_2^{rot_q}(LF) = \{\mathbf{M}^q, \mathbf{D}^q, \mathbf{Q}^q\} = \{\{d_0\}, \{f_{1-1}^q, f_{10}^q, f_{11}^q\}, \{0, 0, q^+, 0, q^-\}\}. \qquad (3.5)$$

L \ M	-2	-1	0	1	2
0			0.282		
1		-0.063	0.226	-0.040	
2	-0.018	-0.012	0.099	-0.066	0.045
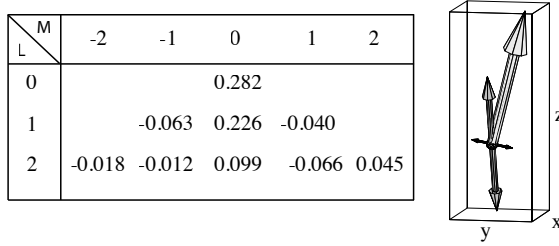
Figure 3.2: Schematic graphical representation of the second order light field. The SH coefficients are presented on the left side. The mutual orientation of the components D, $q+$ and $q-$ is shown on the right side. The length of the light gray arrow corresponds to the value d_1 (strength of the light vector), the lengths of the dark gray and black arrows correspond to values $q+$ and $q-$.

In this case we need only 6 coefficients, the remaining three degrees of freedom being absorbed by the rotation of the axes. Of these 6 coefficients only the 3 that define the monopole and squash tensor will be significant and f^q_{1-1}, f^q_{10}, and f^q_{11} will be close to zero. The structure can be represented graphically as shown in Figure 3.2.

3.2.2 Physical interpretation of the squash tensor

The monopole component d_0, the dipole component $\mathbf{v} = \{f^q_{1-1}, f^q_{10}, f^q_{11}\}$, and the squash tensor component specified by q^+ and q^- are rotationally invariant descriptors of the structure of the light field. The physical meaning of the squash tensor component is most easily grasped in the case that the light vector vanishes. Because the radiance is a non-negative function of direction the monopole component is always necessary. There are two qualitatively different configurations for such a pure quadrupole field. One is the 'light clamp' (therefore 'squash tensor'), which corresponds to the light field between two identical light sources opposite to each other. The other configuration is that of a 'light ring' (Figure 3.3).

<div align="center">(a)   (b)</div>
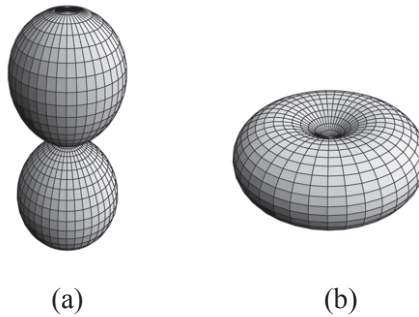
Figure 3.3: Special cases of light fields due to the squash tensor: (a) a light clamp, (b) a light ring. The light vector is assumed to be zero.

3.3 The Plenopter

We have constructed a device that makes it possible to measure the light field up to (and including) the second order as a single observation. The device is roughly spherical with a diameter of 20 centimeters. It can easily be taken outdoors to do measurements in a natural environment. Instead of using cameras with fish-eye lenses we used a number of photo-diodes. This greatly expands the dynamic range at the cost of spatial resolution. We took our inspiration from number of devices proposed by Gershun. Gershun's device for the observation of the light vector consists of a sandwich of photocells in a back-to-back configuration. This device is very similar to ours except for the fact that Gershun divides the sphere into two, we in twelve congruent apertures.

3.3.1 Short description

The second order development in spherical harmonics contains nine free parameters. The simplest regular polyhedron with nine or more faces is the dodecahedron, which has twelve faces. The sphere of directions was divided into twelve mutually congruent pentagonal solid angles. The photocells collect radiation from these apertures, which have a diameter of $2 \times 74.75°$. Diaphragms and a diffuser were placed so as to uniformly integrate over the aperture. The photocells were Siemens BPW21 silicon photodiodes (sensitive from 350 nm to 820 nm) connected to logarithmic amplifiers followed by an AD converter. We obtain a dynamic range of about seven decades. A single observa-
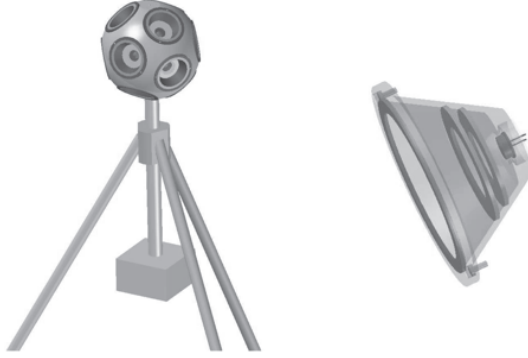
Figure 3.4: Our custom made light measuring device which we named 'Plenopter'.

tion thus yields twelve radiance samples. From this overdetermined sample we find the coefficients of the spherical harmonic development by means of a least squares method. Currently the remaining 3 degrees of freedom are discarded.

3.3.2   The basic data conversion

A single plenopter measurement yields 12 values corresponding to the 12 photocells. The photocells have a certain angular sensitivity profile $S_j(\theta, \phi)$ as a function of the direction of the incident light $LF_j(\theta, \phi)$.

Thus,

$$P_j = \int S_j(\theta, \phi) \cdot LF(\theta, \phi) d\Omega, j = 1, ..., 12, \tag{3.6}$$

where P_j is the output value corresponding to cell j.

The photocells' angular sensitivity profile was measured and decomposed to spherical harmonics, so it can be represented as

$$S_j(\theta, \phi) = \sum_{lm} s_{lm}^j \Upsilon_{lm}(\theta, \phi) + \varepsilon^j \tag{3.7}$$

The shape of the sensitivity profile is the same for all photocells (but may differ by a scaling factor), so once the profile for one of the cells has been measured, all the others can be achieved by rotation and scaling. Furthermore, we can describe the radiance in

terms of spherical harmonics as:

$$LF(\theta, \phi) = \sum_{lm} c_{lm} \Upsilon_{lm}(\theta, \phi) + \varepsilon \tag{3.8}$$

In the sequel we neglect the errors ε. Then, altogether, this results in

$$P_j = \int [\sum_{lm} s^j_{lm} \Upsilon_{lm}(\theta, \phi)][\sum_{l'm'} c_{l'm'} \Upsilon_{l'm'}(\theta, \phi)] d\Omega = \sum_{ll'mm'} s^j_{lm} c_{l'm'} \int \Upsilon_{lm}(\theta, \phi) \Upsilon_{l'm'}(\theta, \phi) d\Omega \tag{3.9}$$

and due to orthonormality of spherical harmonics basis functions

$$\int \Upsilon_{lm}(\theta, \phi) \Upsilon_{l'm'}(\theta, \phi) = \delta_{ll'} \delta_{mm'} \tag{3.10}$$

we finally end up with

$$P_j = \sum_{lm} s^j_{lm} v_{lm} = (\vec{s^j}, \vec{c}). \tag{3.11}$$

If we renumber the coefficients and limit the spherical harmonics approximations to the second order (i.e. $l = 0, .., 2, m = -l, .. l$ altogether 9 coefficients), we get a system of 12 equations with 9 unknowns c_k:

$$P_j = \sum_{k=1}^{9} s^j_k c_k. \tag{3.12}$$

The system is overdetermined, and an approximate solution can be found by means of a least squares technique [22]. The plenopter is $120°$ rotation symmetric, therefore we can get more data for that system rotating the plenopter around its vertical axis. The angular sensitivity profiles for the cells in their new orientations can be achieved rotating the spherical harmonics description $S_j(\theta, \phi)$. Each rotation adds 12 more equations to the system providing more data.

3.3.3 Calibration and tolerances

The basic photo-electric calibration was done in a calibrated solar simulator using a set of calibrated neutral density filters.

There are many processes that lead to systematic and random errors. We investigated the following:

— thermal properties, drift, offset, etcetera of the twelve photo-electric subsystems

— deviations from a curved logarithmic response for the individual subsystems

— the spectral sensitivities of the subsystems

— the precise geometry of the apertures of the subsystems

— possible issues of optical and electrical cross-talk

We used standard methods to investigate these possible issues. We find a mixture of minor systematic and random errors. In the final analysis the instrument can be said to yield correct results within about 5 percents if no special corrections are applied. This was judged to be sufficient for the current application.

The sample frequency is at least 100 Hz. The experiments reported here were essentially static though.

3.4 Empirical light field studies

In the general introduction we hypothesized that the light field can be thought of as a property of the scene geometry. In the present section we describe empirical studies in which we tested this hypothesis by modeling and measuring light fields of a few canonical scene geometries. For negative edge (a long street) and step (a long wall adjacent to a large square) geometries we compared measurements at several points along and accross the streets and walls. We did measurements in three typical narrow streets and one square in the old part of Utrecht. The streets were about 10 meters wide and the buildings alongside the street and square were about 10 meters high. Measurements were taken with a step size of approximately 1m at a height of 1.5m. We tested under clear sky and under overcast sky conditions, so the primary light sources were the sun (if not occluded) and the visible part of sky (which forms a stripe). If our hypothesis is right, the measurements along the streets and walls should be constant up to minor non-systematical differences, while those accross the streets and walls should change systematically and smoothly. Secondly, we modeled these qualitative aspects of the second order approximations.

In order to demonstrate the influence of albedo we also compared measurements and models for an indoor scene with a black and with a white wall. For this purpose we used a laboratory room 6×5 meters with a window on the wide side and matte black side walls and ceiling, facing North. So, here the primary light source was only the part of the sky that was visible through the window. We considered two situations: the wall opposite the

window was covered by white or black paper. Measurements were taken over an array of 9 points at a height of 1.5m, 1.5m apart in one direction and 1.25m apart in the other direction.

A complete set of measurements took about 15 minutes per scene. The coefficients of the second order spherical harmonic approximations (SH2) were estimated by the over-determined system described in the Plenopter section, via least squares optimization.

3.4.1 Models

For the street and wall scenes we made schematic representations, see Figure 3.5. The width of the street and the height of the walls were measured in the real scenes where the measurements were taken. The walls were assumed to be uniform and infinitely long. The position of the sun and the orientation of the street with respect to the sun were looked up on the basis of the geographical coordinates and measurements times and dates.

The primary illumination in our scenes was due to the sun and sky. For the description of the radiance distribution from the sky and sun we used CIE standard models [23], in the case of a clear sky we used the 'CIE standard clear sky, low illuminance turbidity', and in the case of an overcast sky model the 'overcast, moderately graded and slight brightening towards the sun' model.

Taking into account the low spatial resolution of the second order light field [4] we assume that their properties can be sufficiently captured by very simple models. A second order approximation can be thought of as a low frequency filter which filters out high frequencies introduced by specularities and small albedo variations. Therefore the material properties do not have to be specified in detail. For simplicity we assume them to be Lambertian and uniform with albedo 0.1, which is an average albedo for urban scenes [24].

The models were implemented in Mathematica 5.2. We took into account up to two interreflections.

3.4.2 Results

The second order light fields for the street geometries are shown in Figure 3.6. On the left side we show the predictions from the models, on the right side the actual measurements. The spherical harmonics coefficients for each point were normalized (scaled) by the DC component at that point to allow comparisons between points and between models and
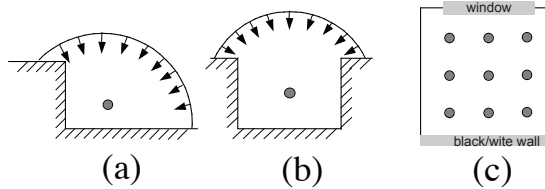
Figure 3.5: Schematic descriptions of the scenes: a) wall, b) street, c) room.

measurements. The results for the three streets a, b and c in clear sky (1) and overcast sky (2) conditions are depicted in different rows. In Figure 3.6(b,1) the sun was directly visible from points 6-9, in all other cases the sun was occluded either by clouds or by buildings. In Figure 3.6 we clearly see that, firstly, the measurements change very smoothly and systematically as a function of position in the scene; secondly, the global structures of the light fields are very similar for the measurements and simple models; thirdly, the global structures of the light fields are very similar for the different streets.

Figure 3.7 shows the measurements for the wall geometry. The top row shows results for a clear sky, the bottom row for an overcast sky. The sun was not directly visible in neither cases. Here we also see very smooth and systematical behavior of the light field. In Figures 3.6 and 7 we can see a clear difference between overcast and clear sky conditions. Under a clear sky the light vector is stronger and aligned with the positive component of the quadruple, whereas the negative component of the squash tensor is quite small. However in the case of an overcast sky the negative component of the squash tensor becomes larger (the light field is more diffuse).

Figure 3.8 shows the measurements for the room scene of which the wall opposite to the window was matte white (a-b), or matte black (c-d). In the left half we depicted views from above (a and c), and in the right half side views (b and d) of individual measurements. The window was located near points 1-3. The results for the white and black walls look very similar, however the magnitudes of the light vectors and the squash tensors show clear and systematic differences, especially at the points which are closer to the back wall, see Figure 3.9: the absorbtion of the black wall results in a relatively stronger dipole component.
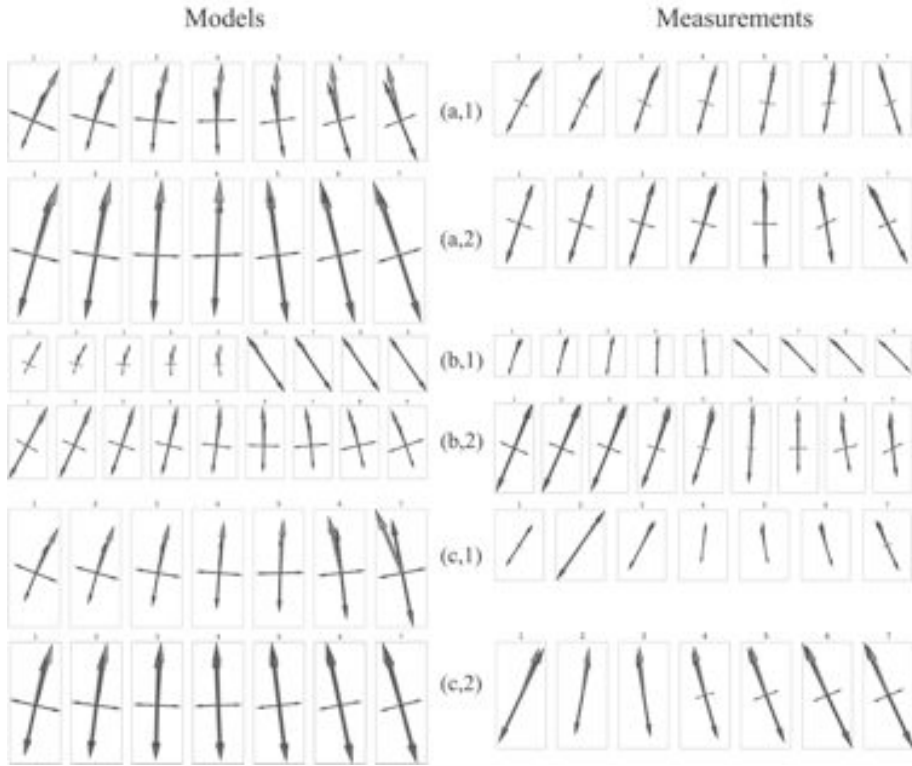
Figure 3.6: Comparison between models (left) and measurements (right) for 'street scene' configurations. The vectors represent the light field up to the second order (see Figure 3.2). We considered from 7 to 9 points per scene (depending on the scene dimensions).

3.5 Discussion

The measurements clearly indicate that in scenes of similar geometry the light fields demonstrate characteristic variations of the light vector and the squash tensor over the scene. This happened despite the fact that the streets possessed different reflective properties and even were differently oriented with regard to the primary light sources (the sun). So these results are in line with our hypothesis that in scenes of similar geometrical layouts one should expect to find qualitatively similar low order light fields and in that

45

(a)

(b)
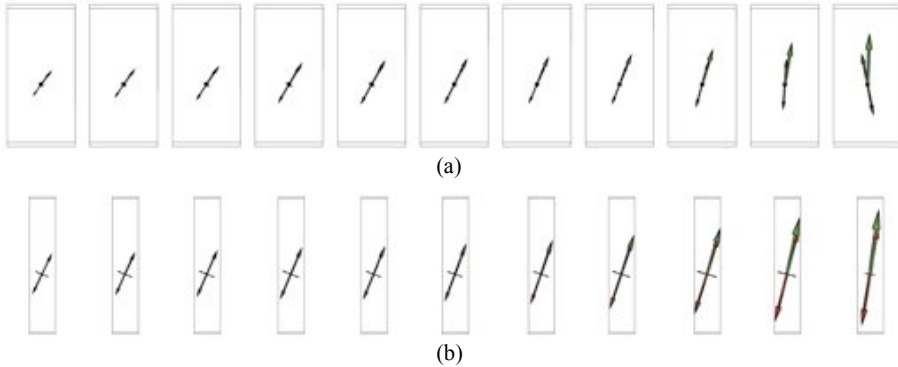
Figure 3.7: Measurements of second order light fields for the 'wall' scene (a) in the case of a clear sky, and (b) in the case of an overcast sky. The sun was not visible in neither cases.

sense the light field can be thought of as a property of the geometry.

Although there are some deviations between our simple model predictions and the actual measurements, the correspondence between them is evident. The main difference concerns the negative components of the –approximately horizontally oriented– quadruples which tend to be larger in the theoretical predictions than in the measurements for the wall and street scenes. This may be due to the fact that in the models we assumed the materials to be Lambertian and uniform, while real materials may scatter light in different ways. For example, backscattering of rough surfaces [25] or (off-)specular scattering tend to result in angular distributions of the scattered radiance which are centered around the illumination direction and specular direction, respectively. In combination with a primary light source from above, this may result in a relatively smaller contribution from reflections of the walls and therefore smaller quadruples.

The measurements in the room scene (Figure 3.8) confirm that the secondary light sources are much less significant than the primary illumination and geometry. The main differences between the white and black wall conditions concern the points which are just next to the wall. Note that in real scenes albedo variations usually are much less extreme. Thus, the smooth and systematic behavior of the low orders over the scene suggests that similar patterns may be found in any other scene with a similar geometry (assuming the

46
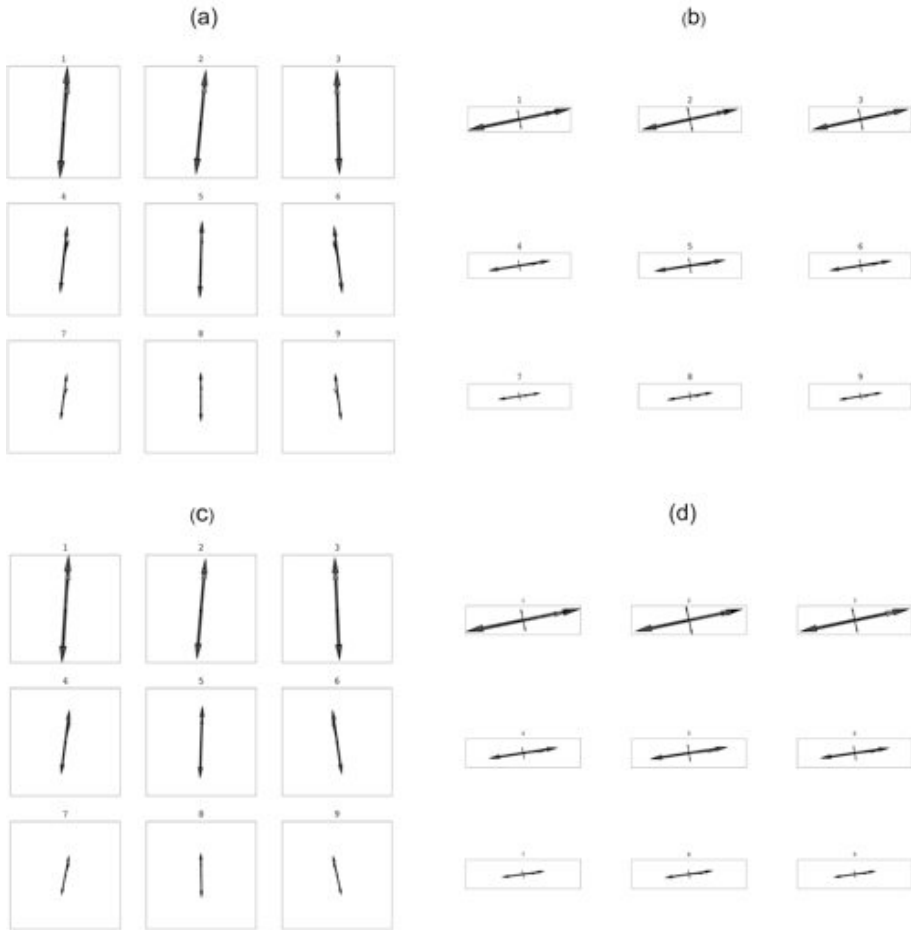
Figure 3.8: Measurements for the 'room' scene. (a)-(b) white wall, (c)-(d) black wall, (a) and (c) view from above, (b) and (d) view from a side.

light comes only from the window).

In this paper we presented a new technique to capture the global structure of the light field in terms of spherical harmonical functions. Existing techniques to capture the light field, the photic field, the plenoptic function, or the Lumigraph [26] result in representations with a much higher angular resolution. These techniques are very useful for high quality renderings of scenes which include small and glossy objects. However,

47
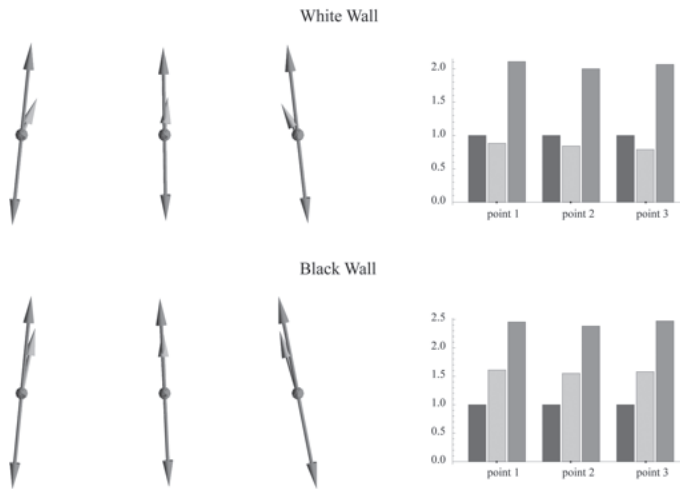
Figure 3.9: Room scene. At the left we show the vector representations for the points near the wall for the white and the black cases. At the right we show the ratios of the magnitudes of the mono-, di- and quadruples with the monopole.

our technique is sufficient for scenes with large matte objects and provides a potentially very high spatial resolution (the number of points at which plenopter measurements are taken may be very high - individual measurements including placement of the apparatus just take a minute) in combination with an extreme high dynamic range up to 7 decades (note that simple photographic techniques can never cover this dynamic range). Moreover, our technique provides insight into the global structure of light fields. This may help to understand what, for instance, a 'natural complex light field' [11, 12, 13, 14] actually means and check whether the hypotheses about it ([27, 28, 29, 30]) are true. These insights into the global structure of natural light fields are important for fields which involve the perceptual qualities of the illuminance environment, such as architecture, interior design and illumination engineering.

BIBLIOGRAPHY

[1] A. Gershun, 'The light field,' J. Math. Phys. **18**, 51151. (1939) (translated by P. Moon and G. Timoshenko).

[2] P. Moon, D. E. Spencer, *The Photic Field*, (MIT Press, 1981).

[3] R. Ramamoorthi, and P. Hanrahan, 'On the relationship between radiance and irradiance: determining the illumination from images of a convex Lambertian object,' J. Opt. Soc. Am. A. **18(10)**, 2448-2459(2001).

[4] A.A. Mury, S.C. Pont, and J.J. Koenderink, 'Light field constancy within natural scenes,' Applied Optics **46(29)**, pp. 7308-7316, 2007.

[5] C. Cuttle, *Lighting by Design*, (Architectural Press, 2003).

[6] C. Cuttle, 'Lighting Patterns and the Flow of Light,' Lighting Research and Technology **3(3)**, 171-189, (1971).

[7] L. Michel, *Light: the shape of space* (John Wiley, 1995).

[8] T. S. Jacobs, *Drawing with an Open Mind* (Watson-Guptill, 1991).

[9] M. Baxandall, *Shadows and enlightenment* (Yale University Press, 1995).

[10] A. Adams, *The negative* (Little, Brown and Company, 1981).

[11] R.O. Dror, T.K. Leung, E.H. Adelson, and A.S. Willsky, 'Statistics of Real-World Illumination,' in *Proceedings of the IEEE Computer Society Conference on Computer Vision and Pattern Recognition*, (IEEE, 2001), pp. 164-171.

[12] R. W. Fleming, R.O. Dror, E. H. Adelson, 'Real-world illumination and the perception of surface reflectance properties,' J. Vision **3**, 347-368 (2003).

[13] R.O. Dror, A.S. Willsky, E.H. Adelson, 'Statistical characterization of real-world illumination,' Journal of Vision **4**, 821-837, (2004).

[14] J. Huang, D. Mumford, 'Statistics of Natural Images and Models,' in *Computer Vision and Pattern Recognition* (IEEE, 1999), pp. 541-547

[15] S. Teller, M. Antone, M. Bosse, S. Coorg, M. Jethwa, and N. Master, 'Calibrated, registered images of an extended urban area,' in *Proc. IEEE Computer Vision and Pattern Recognition* (CVPR, 2001), pp. 93-107.

[16] E. H. Adelson and J. R. Bergen, 'The plenoptic function and the elements of early vision,' in Computational Models of Visual Processing, M. Landy and J. A. Movshon, eds. (MIT Press, Cambridge MA, 1991), pp. 3-20.

[17] J. D. Foley, A. van Dam, S. K. Feiner, and J. F. Hughes, *Computer Graphics, Principles and Practice*, (AddisonWesley Publishing Company, Reading, Massachusetts, 1990).

[18] W. Metzger, *Gesetze des Sehens,* (Kramer, Frankfurt, 1953).

[19] C.J. Copi, D. Huterer, D.J. Schwarz, G.D. Starkman, 'On the large-angle anomalies of the microwave sky,' Mon. Not. R. Astron. Soc., 1-27, (2005).

[20] M.R. Dennis, K. Land, 'Probability density of the multipole vectors for a Gaussian cosmic microwave background,' Mon. Not. R. Astron. Soc., 424-434, (2008).

[21] J.J. Koenderink, A.J. van Doorn, 'Geometrical modes as a general method to treat diffuse interreflections in radiometry,' J. Opt. Soc. Am. **73(6)**, 843-850, (1983).

[22] Press et al, *Numerical Recipes in C*, (Cambridge University Press, 1988).

[23] S. Darula, R. Kittler, 'CIE General Sky standard defining luminance distributions,' in *Proceedings ESim conference*, (IBPSA, Canada, 2002), pp. 1113.

[24] Akbari, H., L. S. Rose, and H. Taha, 'Characterizing the Fabric of the Urban Environment: A Case Study of Sacramento, California,' LBNL-44688, Lawrence Berkeley National Laboratory, Berkeley, California, 1999.

[25] S.C. Pont, J.J. Koenderink, 'Reflectance from locally glossy thoroughly pitted surfaces,' Computer Vision and Image Understanding, **98(2)**, 211222, (2005).

[26] S. J. Gortler, R. Grzeszczuk, R. Szeliski, and M. F. Cohen, 'The lumigraph,' in *Computer Graphics, Proc. SIGGRAPH96*, (1996), pp. 43-54.

[27] H.M. Fox, G. Vevers, *The nature of animal colours. Sidqwick and Jackson*, (The Macmillan Company, 1960).

[28] D. Gomez, M. Thry, 'Simultaneous crypsis and conspicuousness in color patterns: compara-
      tive analysis of a Neotropical rainforest bird community,' The American Naturalist, **269**, 42-61,
      (2007).

[29] G.H. Thayer, *Concealing Coloration in the Animal Kingdom*, (Macmillan, 1909/1918).

[30] J. A. Endler, 'The color of light in forests and its implications,' in *Ecological Monographs 63*
      (Ecological Society of America, 1993), pp.1-27.

CHAPTER 4

REPRESENTING THE LIGHT FIELD IN FINITE 3D SPACES FROM SPARSE DISCRETE SAMPLES

Abstract

We present a method for measurement and reconstruction of light fields in finite spaces. Using a custom made device called Plenopter we can measure spatially and directionally varying radiance distribution functions from a real-world scene up to their second order spherical harmonics approximations. Interpolating between measurement points we can recover this function for arbitrary points of a scene. We visualized the global structure of the light field using light tubes which gives an intuitive description of the flux propagation throughout 3D scenes and provides information about the quality of light in the scenes. Our second order reconstructions are sufficient to render convex matte objects and therefore have a direct interest for computer graphics applications.

4.1 Introduction

The radiance distribution throughout the empty space of a 3D scene is a complicated function and therefore rarely mapped out empirically. However, knowing the light field [1], [2] of a real scene (or at least some of its qualitative properties) is important for many applications: an interior designer can predict the appearance of an object placed at some arbitrary point in that scene, an architect can make a decision whether the building satisfies the standards. In computer graphics the light field is important for rendering purposes - imagine an object moving through a scene, its appearance changes due to illumination variations along its trajectory. The complexity of the light field makes it difficult to measure and analyze it even at a point. Recovering this function for every point of a finite 3D space is a challenging and tedious (but not impossible!) task. However, the complete description is overkill for most applications. Instead, we limit the description of the structure of the light field to components which are the most qualitatively important for object appearance and which suffice to represent the flux distribution throughout the scene. This simplification allows us to develop a description which gives a clear understanding of the structure of the light fields in 3D scenes.

Quantitative assessment of the visual quality of the luminous environment is typically concerned with measuring illumination incident on surfaces [3], [4]. The radiance distribution in the empty space of a scene is rarely taken into account. The empirical analysis of the structure of light fields in empty space is usually limited to measuring the space illumination of radiation and the light vector at a point [3], [4], [5], [7]. In general, radiant flux propagates from light sources to light absorbing surfaces (however in some special cases, which rarely occur in real scenes, flux lines can be closed). Although it does not produce any visual effect in empty space, the distribution of radiance explains the "spatial and form-giving character" of light. Knowing the radiance distribution one could predict the appearance of a hypothetical object placed somewhere in space and calculate irradiance patterns over its surface.

In this paper we present a new way of measuring and analyzing the structure of light fields in finite 3D spaces. Our custom made device called the Plenopter is capable of measuring local light fields up to the second order in terms of spherical harmonics. This extends the conventional description by a new parameter - the squash tensor (the second order harmonic, [8]). Taking into account that the low order components of light fields in natural scenes typically vary slowly and rather systematically with location [8], the

second order approximation of the radiance distribution function can be estimated reasonably well for all points of the scene using interpolation between a limited number of observations. In order to describe the global structure of the light field of a scene we utilize the concept of light tubes, which provides an easy and intuitive understanding of the propagation of radiant flux throughout the scene. Although this concept is not new [1], it has never been used for applications before.

We applied this method to several simple and complicated light fields. We rendered objects in those scenes in order to make a connection between our formal description and object appearance.

4.2 Previous works

The first theory about the light field was developed by Gershun[1]. In this classical work on photometry he considered the light field in empty space. The complete description of the local light field at a certain point in space is given by the radiance distribution $R(\vartheta, \varphi)$ (*brightness-distribution solid*, according to Gershun) which is a spherical function representing the radiance arriving at the point from all directions. Gershun considered the light field as a vector field in 3D space. The most basic property of the local light field is a scalar parameter, namely the space illumination $d = \int_{4\pi} R(\vartheta, \varphi) d\omega$. The vector characteristic of the light field is called the *light vector* and is given by $v = \int_{4\pi} R(\vartheta, \varphi) d\omega$. The direction of the light vector coincides with the direction of maximum flux transfer and the magnitude is the flux density in that direction (i.e. the difference in irradiance of the two sides of a hypothetical infinitesimal diaphragm). Knowing the light vector at any point in space one can describe the structure of flux transfer throughout space by constructing flux lines which are tangential to the light vector. Flux lines are curved lines in 3D, they typically originate on light sources and end on light absorbing surfaces. Figure 4.1 shows the flux lines calculated for an artificial street scene with buildings on both sides, under uniform overcast illumination; the walls were assumed to be Lambertian with constant albedo, the flux lines in the areas which are not exposed to the primary light source are due to inter-reflections. Such a diagram gives an immediate impression of the flux distribution throughout the scene and also provides indirect information about the illumination on surfaces - the denser the flux lines the stronger the illumination. Gershun [1] considered several cases of light fields theoretically and using calculus he derived light fields for generic light sources like an infinite luminous stripe and a wall. But he never applied the
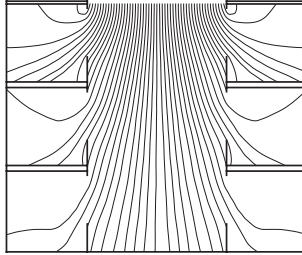
Figure 4.1: An example of flux lines - the distribution of the flux lines inside two three-story buildings opposite to each other (shown as cross-sections) under an overcast sky. The flux lines start at the overcast sky and enter the buildings through the windows. The inter-reflections are taken into account.

concepts of light vector and flux lines to describe lighting conditions in real scenes - at his time such empirical analysis was difficult to realize practically.

In computer science the light field is known as the Plenoptic function [9] which is a function $L(x, y, z, \vartheta, \varphi, \lambda, t)$ of 7 parameters which are position, direction, frequency and time. A recently developed technique [10] allows to photographically capture a simplified 5D plenoptic function $L(x, y, z, \vartheta, \varphi)$ over a certain region of space by recording intensities of all rays passing through the scene. The resulting light field is used in computer graphics for rendering applications [11]. This method exploits the idea that the radiance of a ray is constant along its direction. The disadvantage of this so-called Lumigraph method is that the measurement procedure is rather complicated and that the post-processing involves analysis of huge amounts of data. However, up to now this is the only method of measuring global light fields within finite spaces of real 3D scenes.

A local light field at a point in empty space can also be acquired by means of high dynamic range panoramic imaging [12], [13]. Unger et. al.[14] suggested to use an array of mirror balls in order to capture spatially and directionally varying incident light fields over 2D areas and then extrapolate these data to a volume above the area. These methods are used for modeling light fields for image based rendering applications in computer graphics.

Practically, detailed descriptions of light fields are needed only for rendering highly reflective mirror-like materials. However for most materials high frequency lighting is not necessary because it will be blurred by diffuse scattering of the illuminated object
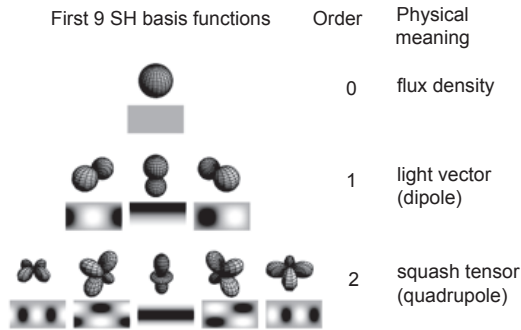
Figure 4.2: The first 9 spherical harmonics basis functions.

(a smooth BRDF works as a low pass filter). This effect has been shown empirically [15],[16] and has been derived theoretically - the second order spherical harmonics approximation of local light fields suffices to render convex Lambertian objects [17],[18]. Moreover, such low order approximations allow to derive the most salient qualitative features of the light field, such as the overall levels and directions of the illumination. The 0th and 1st order components have direct physical meanings, namely the space illumination and the light vector. The 2nd order contribution is more complicated and can correspond to different shapes of brightness distribution solids from a 'light clamp' to a 'light ring'. It is referred to as a 'squash tensor' [8]. In natural scenes the low order contributions to light fields show very systematic and smooth behavior varying very slowly from one point of the scene to another [8],[19].

The field of knowledge that deals with the formal quantifiable assessment of the visual quality of the environment is lighting engineering. A large number of measurable parameters are being used to judge the suitability of the illumination for visual tasks the observer may encounter, e.g. illuminance values, cylindrical illuminance, daylight factor etc [4], [3]. However, lighting engineers are mostly concerned with the illumination incident on surfaces and rarely interested in the radiance distribution in empty space, which is an important factor in the visual assessment of the environment [6]. Up to our knowledge there is only one commercially available device which can be used for measurements of the light vector and space illumination [7].

Light fields in empty space are also important in architecture and interior design. In this field a more artistic approach is used to estimate "spatial and form giving effects" of

lighting. Sample objects are frequently used and the quality of light is judged from the effects that light field cast upon those objects. Cuttle [4] suggested to use three kinds of sample objects - a matte sphere, a black shiny sphere and a disk with a peg in order to reveal shading, highlights and shadow patterns.

Another way of analyzing illumination is via computer modeling. Physically based rendering systems [20] provide tools to calculate and analyze any parameter of the light field. For instance one can calculate the light vectors at points of a regular grid. Visualization of those vectors provides a quantitative description of the flux transfer throughout the scene [21], however this method has certain drawbacks. Light vectors at discrete points do not reveal a global description of the flux transport. Besides, an image consisting of projections of 3D vectors on a 2D image plain is visually ambiguous and therefore it is difficult to grasp correct orientations and magnitudes of the light vectors from such a representation unless all the vectors are coplanar and lay in the image plane. We suggest another method of depicting flux through a 3D scene by visualization of light tubes. This not only gives continuous (along a flux line) information about the light vector, but also makes it easier to see variation of its orientation and strength in 3D.

The irradiance volume [22] is a method of recovering the *irradiance distribution solid* for any point within a virtual scene by means of interpolation. It exploits the idea that the irradiance distribution function (a spherical function representing the irradiance on a hypothetical plane for all possible orientations of that plane) is smooth and therefore easy to interpolate. We use a similar approach and apply interpolation to recover second order approximations of the radiance distribution functions at all points within a certain volume.

4.3   Empirical studies

The goal of our empirical studies is to reconstruct the light field up to the second order approximation at any point inside a 3D space of a scene and to provide insight into the global structure of the light field. We considered several light fields and provide a detailed description of the second order approximations of those light fields. We use a custom made device called Plenopter (Figure 4.3). The plenopter contains 12 high dynamic range sensors in a regular dodecahedron configuration. Each sensor has a large field of view of $74°$ such that altogether they cover the entire sphere, capturing light which is coming to its center point from all directions. Each sensor provides one value representing an average intensity over the field of view. The sensors are radiometrically calibrated. The

Figure 4.3: The Plenopter, a light measuring device capable of capturing local light fields up to the second order. 12 photocells with wide apertures of $74°$ cover the entire sphere capturing light from all directions.

Plenopter is capable of measuring the structure of the local light field up to the second order in terms of spherical harmonics. From a single plenopter sample (12 values) we can calculate 9 spherical harmonic coefficients representing the zeroth, the first and the second order contributions at the measurement point.

The empirical studies were conveyed in the Light Lab (Philips Research) which is a typical empty office room 4 by 6 by 3 meters, equipped with a large number of different kinds of light sources that could be controlled remotely. The equipment of the Light Lab allowed to generate 24 qualitatively different light fields. We applied our analyses to all of them but here show only four which represent the most extreme cases. Schematic outlines of the scenes and photographs of a mirror ball taken in the middle of the room are shown in Figure 4.4. The light sources of the first scene (a) were three square area light sources on the ceiling close to the left wall (Figure 4.4(a)). In scene (b) there was one large diffuse circular light source in the middle of the ceiling (Figure 4.4(b)). The illumination of scene (c) consisted of four spot light sources positioned at the corners of the room and directed downwards (Figure 4.4(c), notice large bright areas on the walls and floor which are directly illuminated). In scene (d) we used three area light sources of the same kind as in the first scene, but in a triangular instead of a linear configuration (see Figure 4.4(d)).

The measurement procedure was as following. We took 45 plenopter measurements
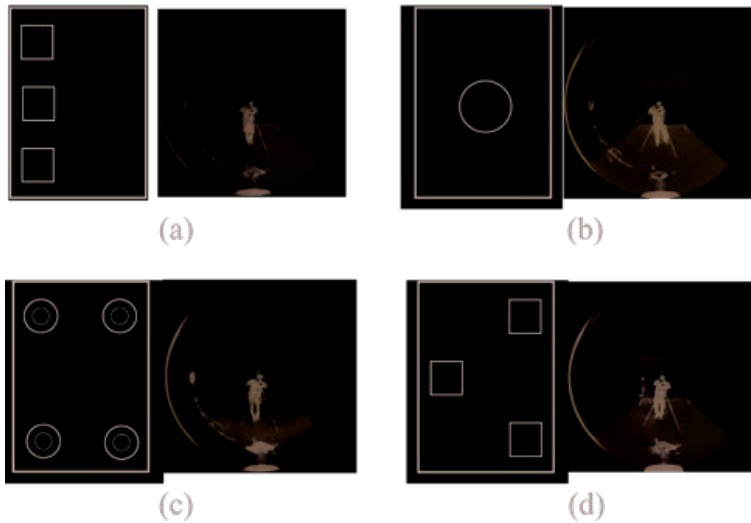
Figure 4.4: Schematic description of the light sources (view from above) and panoramic photographs of the Light Lab for different lighting installations (a) - three diffuse area light sources on the ceiling along the left wall; (b) - large circular diffuse area light source in the middle of the ceiling; (c) - four small spotlights (close to collimated) at the corners on the ceiling directed straight downwards; (d) - 3 diffuse area light sources on the ceiling in a triangular configuration.

over a regular grid at three height levels (100cm, 155cm and 210cm). At each level there were 15 points (array 3 by 5 points) 1m apart. For scenes (a) and (d) the middle level was again measured a few months later, on a finer grid, in order to check the repeatability of the measurements and to find out how good the interpolation is by comparing interpolated data with real measurements at extra points. For any point inside the space enveloped by the measurement points the light field was calculated by means of linear interpolation of the coefficients between the neighbour measurement points.

4.4 Results

Figure 4.5 shows contour plots representing the magnitudes of the first three harmonics (space illumination, light vector and squash tensor) over the plain at a height of 155 cm

(middle level) for all four scenes. The white circles indicate the 15 measurement points taken on this level. Notice that the values of space illumination nicely correspond to the layouts of the scenes (Figure 4.4), the closer to the light source the stronger it gets. Typically, the distributions of the magnitudes for the vectors are similar to those of the space illumination (Figure 4.5). However, in general that does not always have to be true.

The light vector may vanish in points where the local light fields are symmetrical, for instance in the middle between two identical light sources. The structure of the squash tensor and its behavior is more difficult to interpret than the previous two, in fact the higher the order the more complicated it gets. However, there are two canonical cases of the squash tensor which could be named "light clamp" and "light ring" that have simple geometrical interpretations and can help to understand the behavior of the squash tensor. For instance, in the middle of scenes (a) and (d) the squash tensor has local maximums which, as we can judge from the geometrical layouts of the scenes are due to a strong "light clamp" in those points.

In order to test how good the interpolation is we took eight extra measurements in between the grid points for scenes (a) and (d). The locations of extra measurements are indicated by black crosses in Figure 4.5(a) and 4.5(d). Figure 4.6 shows the comparison of the 9 spherical harmonics coefficients calculated from real measurements (light gray bars) at those extra points against coefficients calculated by using interpolation (dark gray bars) on the basis of the 45 original samples. As we can see the measured and interpolated coefficients correspond rather well even for scene (d) which is structurally complicated; mean correlations between the vectors of interpolated and measured SH coefficients were 0.89 for scene (a) and 0.92 for scene (d). The errors can be partially explained by the large step-size of the grid - we used $3 \times 5 \times 3$ grids with a step of 1m. Obviously, complicated light fields which consist of rather collimated light sources with beam widths of tens of centimeters (like scene (c)) would require a finer grid. There are also errors due to the misplacement of the device, the accuracy of the plenopter's location was ± 5cm in 3D. At special points of the light field, for instance on the light-dark edge in the case of collimated light, such misplacement of the device could lead to significant errors.

It is rather difficult to understand the shapes of the light fields purely from the coefficients and therefore Figure 4.7 shows panoramic pictures ($360° \times 180°$) which represent the spherical radiance distribution functions up to the second order approximations, corresponding to the coefficients shown in Figure 4.6. Figure 4.7 demonstrates that the interpolated spherical functions capture the qualitative structure of local light fields very well,
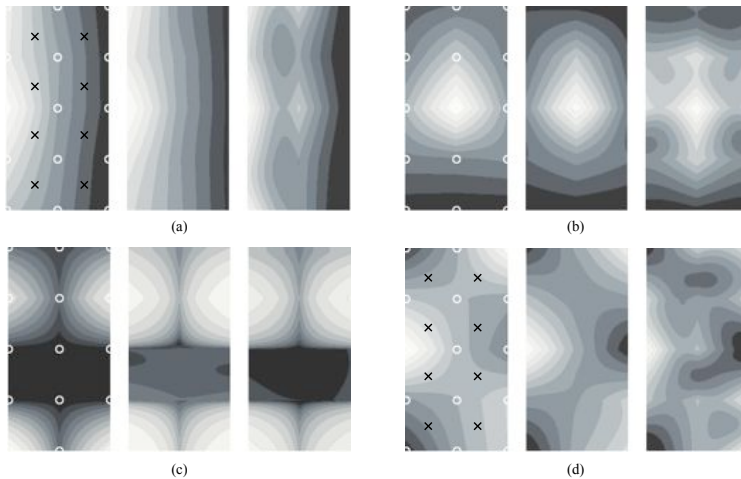
Figure 4.5: Logarithmic contour plots representing the magnitudes of space illumination (left), light vector (middle) and squash tensor (right) over the middle level (155 cm) for scenes depicted in Figure 4.4. The magnitudes were scaled individually such that the maximum range of gray values is used. White crosses indicate the measurement points which were used for interpolation, black crosses indicate the extra measurements taken in scenes (a) and (d).

notice that bright and dark patches on contour-plots corresponding to measured and inter-polated coefficients coincide. So, although the errors in the individual spherical harmonic coefficients sometimes are large (Figure 4.6), they hardly ever lead to serious errors in the global structure of the second order approximation of the spherical function, which is the summation of all 9 spherical harmonics basis functions weighted by the coefficients.

Figure 4.8 shows the light tubes for all four scenes. The light tubes are constructed in such a way that they are always tangential to the light vector and the radius of the tubes is inversely proportional to the magnitude of the light vector $r = 1/\sqrt{\pi\|v\|}$, meaning that the flux through orthogonal cros-sections of the tube is constant. It is useful to think of the light flux through the light tube as of incompressible fluid flow through a tube - the amount of flux through an element of the tube is constant independently of the width of that element, however the speed varies inversely proportional to the radius of the tube. In this case the magnitude of the light vector is analogous to the flow velocity. In Figure
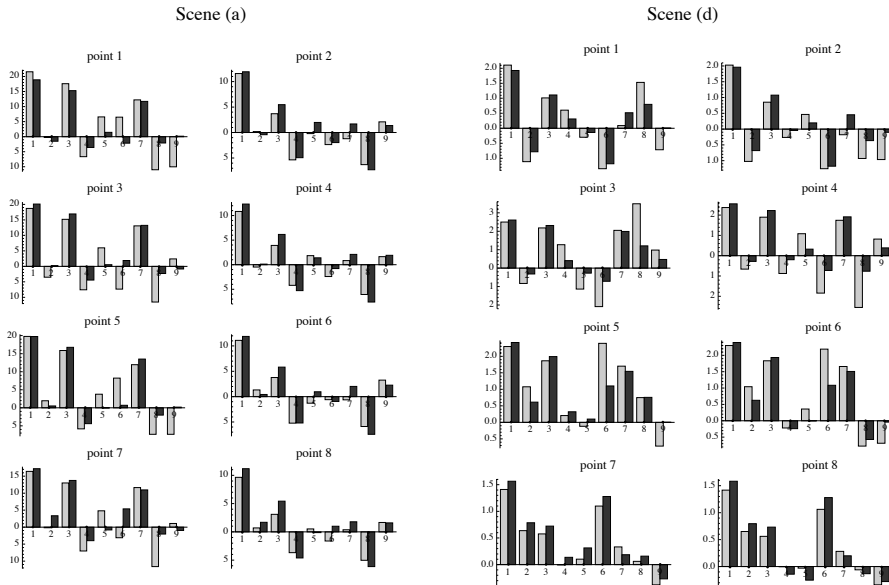
Figure 4.6: Spherical harmonics coefficients calculated in scenes (a) (left) and (d) (right) at extra points indicated by crosses on Figure 4.5. Light gray bars represent spherical harmonics calculated from real measurements and dark gray from interpolated values.

4.8 drawn squares and circles on the ceiling indicate the light sources, notice that the light tubes correspond very well to the schematics in Figure 4.4. The overall qualitative descriptions of the flux transfer by light tubes are captured correctly for all scenes, as we can judge from the geometrical layouts of the scenes.

In order to capture all flow features a seed placement strategy for the flux lines should be chosen wisely [23]. The resulting image of the light tubes depends on this choice. For instance, if for scene (c) we would have chosen starting points on the left or right walls then perhaps none of the constructed light tubes would have passed through the middle of the room (notice that there are almost no tubes ending on the walls) and therefore the flow pattern in that area would be missing in such visualization. This problem usually occurs around critical points of the field. We have chosen a 5×9 array of points on the ceiling for all the scenes because the flux lines typically originate at the light sources (on the ceiling in our case).

Notice that in scene (c) some light tubes are curved as parabolas starting at the ceiling

Measured   Interpolated

Scene (a)

Measured   Interpolated
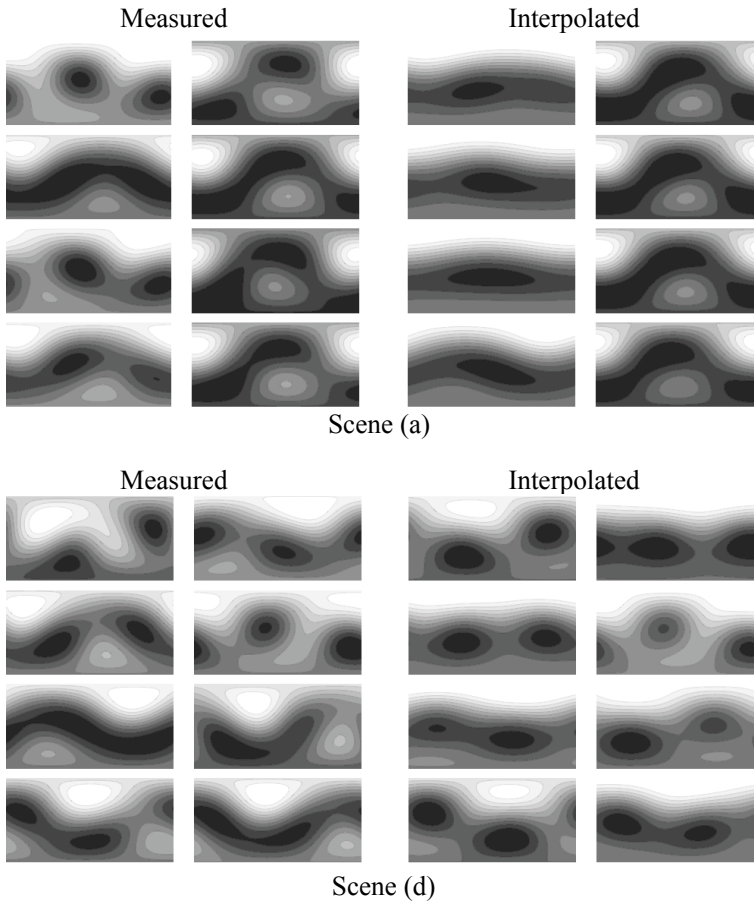
Scene (d)

Figure 4.7: Panoramic $180° \times 360°$ plots representing second order approximations of the light fields corresponding to the coefficients in Figure 4.6 (left - real measurements, right - interpolated) for scenes (a) and (d).

and ending on the ceiling, meaning that the light vector changed its direction almost $180°$. In the middle of that scene the direction of flux transfer is upwards due to strong reflections from the ground. The flux in the upper middle part of scene (c) is very low (light tubes are thick) because the light field there is mostly due to secondary light sources, the strong narrow beams of the primary light sources do not reach that part of the room.

(a)

(b)

(c)

(d)
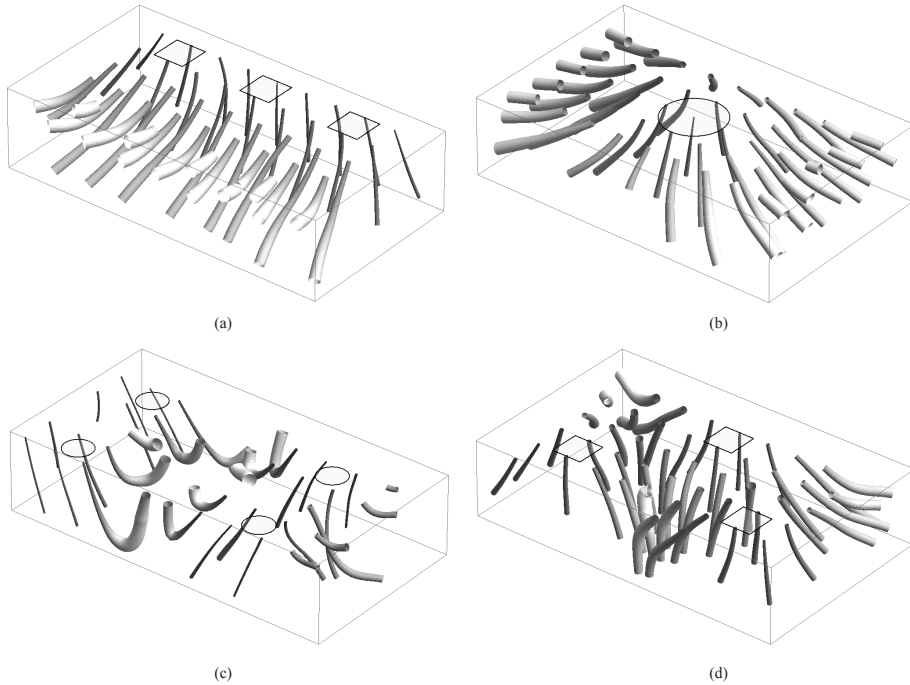
Figure 4.8: Light tubes for the scenes which were schematically depicted in Figure 4.4. The light sources are indicated by squares and circles. The tubes describe radiant flux transfer - flux through any section of any light tube within a scene is constant, the light vectors are tangential to the tubes and their magnitudes are counter proportional to the square areas of tubes sections.

The light tubes provide an intuitive visualization of the light field behavior over the scene and of how the flux propagates through the scene, however they do not provide direct information about the space illumination and the squash tensor. Figure 4.9 shows how the full second order approximation of the light field varies along a tube. We have chosen one light tube from scene (c) (Figure 4.9(a)) and considered 3 points along that tube. Figure 4.9(b) shows the corresponding radiance distribution functions up to the second order approximations and images of a Lambertian object (the Stanford Bunny) rendered using those second order light fields. From the appearance of the rendered objects we can clearly see how the primary direction of light changes along the tube. In the lowest part

66

(a)   (b)
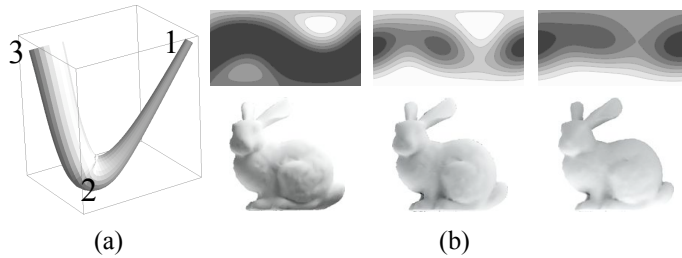
Figure 4.9: Object's appearance along a light tube, (a) - one of the light tubes selected from scene (c); (b) - pictures of Lambertian 3D object (Stanford Bunny) rendered using light fields at points indicated on the tube, the contour plots represent $180° \times 360°$ panoramic images of the second order light fields at those points.

of the tube there is a clear "light clamp" structure - notice that the light field at that point has two maximums which are opposite to each other. The clamp is also visually apparent from the object's appearance.

4.5   Discussion and conclusions

We presented a new technique of measuring light fields and recovering the second order approximation over a finite region of 3D space. Our second order spherical harmonics approximations provide quantitative mathematical descriptions of important structural features of the light field which allow to approach the "spatial and form giving effects" of lighting formally. The major contribution is the possibility to estimate the light field not only locally at a point of space, but globally over the entire space.

We can think of many applications for our technique. Since the light tubes describe the flux propagation throughout a 3D scene it is a useful addition to the tools of lighting engineers. Light tubes provide a qualitative description of the global structure of light fields and also contain quantitative information about the strength of the light vectors. Although light tubes do not give direct information about the space illumination, some information about the space illumination can be retrieved from the light tubes indirectly. Typically there is a correlation between the density of the flux lines and local maximums of space illumination (this does not hold for singular points, for instance where the light vector vanishes). In addition to measuring these well known structural features of the

light field, our method also allows to estimate the squash tensor. Up to our knowledge the available light measuring devices are capable of measuring only light vector and space illumination locally, therefore the possibility of recovering the higher order structural component (squash tensor) takes us a one step further in understanding the quality of light.

Architects and interior designers may also find this technique useful for evaluating the quality of light in a scene globally. Our method allows to find special points in the light field, for instance where the light vector vanishes and the structure of the local light field is dominated by squash tensor. This is a formal scientific approach to express the quality of light in the scene numerically, whereas the 'flow of light' [24], [4], which is based on object appearance, provides only a qualitative description. Besides, the second order spherical harmonics description can be used as lighting input for rendering systems.

In computer graphics our technique could be used as a cheap and quick alternative to the Lumigraph. The angular resolution of the Plenopter is low, however our method provides the global structure of the 5D light field in a finite space on the basis of just tens of measurements of 12 numbers, which can be done in less than an hour, without a need for much memory space and heavy computations. Moreover, our methods provide direct intuitive insights into the global structure of light fields - which is not the case for high resolution methods such as the Lumigraph.

Our measurements showed that even the structure of the first order component of the light field, which is given by the light tubes, can be rather complicated. Notice that the light vector changes its direction almost 180 degrees (Figure 4.8(c)) starting at the ceiling and ending up on the ceiling as well. Theoretically the flux lines can even be closed! In future research we will investigate possible topological structures of the light field and analyze its singular points. Furthermore, we will study the intriguing relations between human perception of the luminous environment and structural features of the light fields.

BIBLIOGRAPHY

[1] A. Gershun, 'The light field,' J. Math. Phys. **18**, 51-151. (1939) (translated by P. Moon and G. Timoshenko).

[2] P. Moon, D. E. Spencer, *The Photic Field*, (MIT Press, 1981).

[3] P. R. Boyce, *Human factors in lighting*, (New York: Macmillan Publishing Company, 1981).

[4] C. Cuttle, *Lighting by Design*, (Architectural Press, 2003).

[5] C. Cuttle, 'Cubic illumination,' Lighting Research and Technology, **29(1)**, pp. 1-14, (1997).

[6] J.J. Koenderink, S.C. Pont, A.J. van Doorn, A.M.L. Kappers, J.T. Todd, 'The visual light field,' Perception **36**, 1595-1610(2007).

[7] http://www.megatron.co.uk/cim/index.html

[8] A.A. Mury, S.C. Pont, and J.J. Koenderink, 'Light field constancy within natural scenes,' Applied Optics **46(29)**, pp. 7308-7316, 2007.

[9] E. H. Adelson and J. Bergen, 'The plenoptic function and the elements of early vision,' in *Computational Models of Visual Processing*, M. Landy, and J. Movshon, eds. (MIT Press, 1991), pp. 3-20.

[10] S. J. Gortler, R. Grzeszczuk, R. Szeliski, and M. F. Cohen, 'The lumigraph,' in *Computer Graphics, Proc. SIGGRAPH96*, (1996), pp. 43-54.

[11] M. Levoy and P. Hanrahan, 'Light field rendering,' in *Proc. SIGGRAPH 96*, (1996), pp. 31-42.

[12] http://www.debevec.org/Probes/

[13] Paul Debevec, 'Rendering Synthetic Objects into Real Scenes: Bridging Traditional and Image-Based Graphics with Global Illumination and High Dynamic Range Photography,' *Proc. SIGGRAPH 98*, (1998), pp. 189-198.

[14] J. Unger , A. Wenger , T. Hawkins , A. Gardner , P. Debevec, 'Capturing and rendering with incident light fields', in *Proc. of the 14th Eurographics workshop on Rendering*, (2003).

[15] R. Epstein, P. Hallinan, and A. Yuille, '5 Plus or Minus 2 Eigenimages Suffice: An Empirical Investigation of Low-Dimensional Lighting Models,' *Proc. IEEE Workshop Physics-Based Modeling in Computer Vision*, (1995), pp. 108-116.

[16] P. W. Hallinan, 'A Low-Dimensional Representation of Human Faces for Arbitrary Lighting Conditions,' in *Proc. IEEE Conference on Computer Vision and Pattern Recognition*, (1994), pp. 995-999.

[17] R. Ramamoorthi, and P. Hanrahan, 'On the relationship between radiance and irradiance: determining the illumination from images of a convex Lambertian object,' J. Opt. Soc. Am. A. **18(10)**, 2448-2459(2001).

[18] R. Basri and D. Jacobs, 'Lambertian Reflectance and Linear Subspaces,' *Proc. Eighth IEEE Int'l Conf. Computer Vision*, (2001), pp. 383-390.

[19] A.A. Mury, S.C. Pont, and J.J. Koenderink, 'Spatial properties of light fields in natural scenes,' in *Proc. APGV 2007, ACM SIGGRAPH, Spencer S.N. (Ed.)*, (2007), p. 140.

[20] G.W. Larson and R. A. Shakespeare, *Rendering with Radiance: the art and science of lighting visualization,* (Morgan Kaufmann Publishers, San Francisco, 1997).

[21] A. Jacobs, *MSc in Energy, Architecture and Sustainability; European Masters in the Integration of Renewable Energies into Buildings, RADIANCE Course (Advanced)*, (London Metropolitan University, London, 2004).

[22] G. Greger, P. Shirley, P. Hubbard, and D. Greenberg, 'The irradiance volume,' *IEEE Computer Graphics & Applications*, **18(2)**, 32-43 (1998).

[23] V. Verma, D. Kao, and A. Pang, 'A Flow-Guided Streamlines Seeding Strategy,' *Proc. IEEE Visualization*, (2000), pp. 163-170.

[24] C. Cuttle, 'Lighting Patterns and the Flow of Light,' Lighting Research and Technology **3(3)**, 171-189, (1971).

CHAPTER 5

———

TOPOLOGICAL STRUCTURES OF LIGHT FIELDS

Abstract

In this paper we study the topological structure of light fields. Using the notion of the light vector the light field can be considered as a 3D vector field. We revisit existing theories of the light field and extend it by considering possible generic topological structures of the flux lines in empty space. We investigate singular points of the light field, show which kinds of generic topological configurations are possible and illustrate them by modeling. Our analysis shows that all types of critical points of 2D vector fields actually occur in light fields with only minor restrictions. We also consider the global structure of the light field. One of the striking results (in view of the fact that the light 'rays' are straight) is that the flux lines of the light fields can even be closed.

72

5.1 Introduction

Understanding the structure of the radiant power transfer through the environment provides insights into the quality of the illumination and the effect that it makes on the visual appearance of the scene. Scientists and illumination engineers are mostly concerned with light incident on surfaces rather than radiant flux traveling through the scene, because the incident illumination is of immediate practical importance (like in interior design and photography). However before the incident illumination is scattered by a surface of an object the radiant power travels from the light source through the medium. If one desires to predict how an object would be illuminated when introduced in an originally empty space, one needs to consider the light field.

The idea that radiant flux flow can be represented as a vector field has been known for a long time [1, 2], but the structural properties of such flow have never been studied in depth. In this paper we revisit existing theories of the light field as a vector field and investigate the structural properties of the light field by studying the behavior of the flux lines. The primary goal of our study is to investigate what kinds of generic topological structures are possible in light fields and to illustrate the nature of singular points. Qualitatively the vector field can be classified by means of the singular points and by describing the flux lines in their vicinity. We show that all critical points typical for general 2D flow fields also occur in light fields and provide models which illustrate those cases.

5.2 Radiometric preliminaries

The fundamental parameter by means of which all other radiometric quantities may be defined is the radiance - the amount of radiant power emitted from or passing through a unit area in a certain direction per unit solid angle. The luminous environment can be considered as being filled with beams carrying radiant power. Infinitely many rays enter every point in space from all possible directions. A formal description of the luminous environment involves the radiance distribution function $R(x, y, z, \vartheta, \varphi)$ which describes the radiance coming at a point given in Cartesian coordinates (x, y, z) from directions given in spherical coordinates (ϑ, φ). This nonnegative function contains rays of light traveling through all points in the space in all directions and completely defines the distribution of radiant power in the medium. Here we consider stationary, quasi-monochromatic beams (the 'plenoptic function' [3] contains two additional variables, namely the frequency λ

and the time t). We consider incoherent beams throughout the paper.

For applications the amount of radiant power per unit area incident on a surface is generally considered to be an important measure. This quantity is given by the irradiance $I(x,y,z,\vec{n})$ where the orientation of the plane is given by its surface normal $\vec{n} = (\vartheta, \varphi)$. In empty space we can consider the irradiance on a hypothetical plane. Rotating the plane around a point and spanning all directions we can construct the irradiance distribution function at that point. In the computer graphics community this spherical function is known as the irradiance volume [4]; the pre-calculated irradiance volume can be used for rendering a matte object placed at the point, this technique is useful for rendering dynamic scenes.

In order to characterize radiant flux propagation in space let us consider a transparent aperture instead of opaque plane. The flow of radiant power through the aperture is given by the difference of irradiances on both sides of the aperture. This quantity is known as the flux density [1]

$$Dn(x,y,z,\vec{n}) = I(x,y,z,\vec{n}) - I(x,y,z,\vec{-n}).$$ (5.1)

Knowing the radiance distribution function at any point of space we can construct a vector

$$D(x,y,z) = \int_{4\pi} R(x,y,z,\vartheta,\varphi)d\omega,$$ (5.2)

at any point of space. The vector field D is known as the 'light field' and the quantity $\mathbf{D}(x,y,z)$ is referred to as the 'light vector'. It is important to point out the difference between a single 'ray' and the light vector - the light vector is the average at a point over all directions of the entire sphere and therefore it characterizes not the radiance distribution but the net radiant flux flow through that point. The physical meaning of the light vector is that it indicates the direction of maximum transfer of net radiant flux and the magnitude gives the flux density in that direction.

The projection of the light vector on a certain direction gives the flux density through a hypothetical aperture orthogonal to that direction. Thus for area elements that contain the light vector the flux density is zero, irradiances on both sides of an aperture are equal and cancel each other out. Therefore there is no flux through apertures which are coplanar with the light vector. The concept of the light vector finds many applications in illumination engineering - knowing the light field one can calculate the amount of light traveling in space. Solutions of the light vector field due to certain canonical light sources such as an infinite luminous strip, a polyhedral aperture (for instance a door or window) and so

74

on have been developed by many authors [1, 2, 5]. The fact that the light field is a true vector field simplifies the calculations - a light field due to multiple light sources may be obtained as a superposition of light fields due to the individual sources.

5.3 The structure of light fields

The global structure of the light field can be investigated by means of generic mathematical tools designed for vector fields. Knowing the light vector at all points of space we can construct the flux lines which are tangential to the light vector. In general for translucent media without any occluders the flux lines are smooth 3D curves. These curves typically originate at light sources and end on light absorbing surfaces. The radiant flux propagates through space along the flux lines, in the direction of the light vector. For instance for a single point light source the flux lines are straight radial lines diverging from the source.

In order to complete the flux lines with the information about the magnitude of the light vectors, one can construct a 'light tube' of variable radius over the flux line such that the flux through the surfaces of orthogonal sections is the same everywhere along the tube [1, 6]. The radiant flux through a surface is a projection of the light vector on that surface multiplied with the surface area, so the width of the light tube is inversely proportional to the magnitude of the light vector at that point. Notice the similarity between radiant flux transfer and fluid dynamics of incompressible liquid, the magnitude of the light vector is analogical to the speed of the liquid in a tube - the narrower the tube the higher the speed. The boundary of the flux tubes is made of field lines, thus there is no net transport of radiant flux over flux tube boundaries, radiant power is effectively transported by way of the flux tubes. Although the resulting global structure may be rather complicated, visualizations of the light tubes help to understand the flux transfer in 3D space [7].

In this paper we will be primarily concerned with light fields with an axis of translational symmetry which can be easily visualized by flat 2D flux lines. Figure 5.1 shows flux lines of several light fields due to different configurations of point light sources (in 3D they are line sources indeed). The contour plots underneath indicate the magnitudes of the light vectors at corresponding points. Figure 5.1(a) shows the structure of a light field due to five point light sources of equal intensity. Notice that between the middle and the four other sources there are four special (singular) points in empty space where the light vector vanishes - due to the symmetry of the flux density at those points there are no primary directions for radiant power transfer and therefore the light vector is zero. In
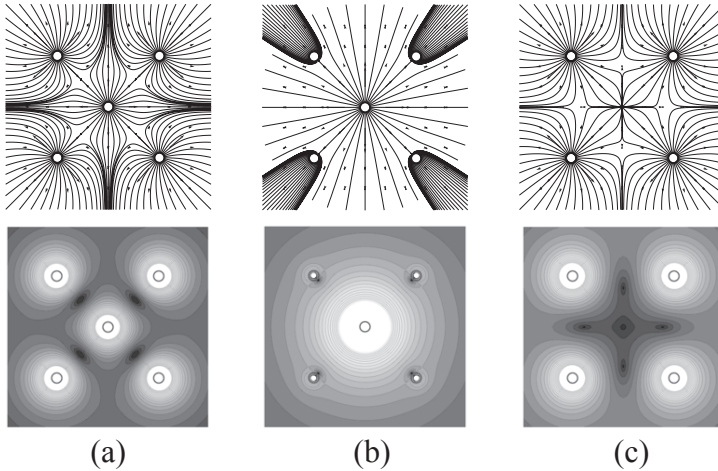
Figure 5.1: Light fields due to point light sources. The upper images show the flux lines, the contour plots underneath indicate the magnitudes of the light vectors

Figure 5.1(b) the light sources have the same geometric configuration but the middle one is much stronger than the others, so the light field of the middle source dominates and 'washes away' the flux lines of the other light sources. However qualitatively the structures of the light fields in Fig 1(a) and Figure 5.1(b) are the same - in both cases there are four singular points of the same type (saddle points) and the flux lines behave similarly. In Figure 5.1(c) we removed the middle light source which added one extra singular point. The qualitative structure of the fields is conveniently characterized by a description of the singular points (light sources or sinks and saddle point) - their locations and qualitative properties. There exists only a limited number of generic qualitatively (topologically) different singular points in vector fields and we will consider which of them may happen in light fields and show examples.

Notice the similarity between the behavior of the light field and the electrostatic field. Flux lines of point light sources are the same as of positive electric charges. These analogies motivated scientists to develop a field theory of the light field in terms of the light vector on the basis of partial differential equations describing a potential [1, 2]. However it must be noted that the physical processes which define light transfer lay in electro-

magnetism and strictly speaking the light field in terms of the light vector (i.e. on the macroscale) does not typically possess a potential. Radiant power transfer is different from electrostatics, liquid flow and other kinds of energy or substance transfer. The major difference is the screening effect - beams may be occluded by an object creating shadow or penumbras. This introduces discontinuities for flux lines on the borders of lit and unlit regions. Although the analogies with other physical processes help to understand the behavior of the light field, they should be treated carefully. Scientists and lighting engineers (who used to think of the light field analogously to fluid dynamics) have drawn flux lines on the basis of limited computations and intuition and frequently made mistakes considering flux lines to be continuous (for instance several mistakes in Gershun's classical book were pointed out recently in [8]). The flux lines are continuous only for unoccluded regions.

There are different ways of measuring the light vector - for instance by calculating the flux density in three orthogonal directions (from measured irradiances of six sides of a cube) and these values give the coordinates of the light vector [9]. The most simple, but quite possibly the most intuitive method is so-called 'grease photometer' [6].

In some sense the light vector is analogous to the Poynting vector which represents the energy flux of an electromagnetic field. It also indicates the direction of maximum energy transfer. The Poynting vector is defined in terms of the electromagnetic field and thus describes all details down to diffraction and interference effects. In contradistinction the light vector is defined as a statistical average over an incoherent field and glosses over details at the scale of the wavelength.

5.4 Two-dimensional topology of the light field

5.4.1 Singular points in 2D vector fields

The critical points in a vector field are the points at which the vector vanishes and thus its direction is not defined. Critical points analysis is a powerful tool to describe the structure of a vector field - knowing the critical points and the behavior of the flux lines connecting them it is an easy matter to reconstruct the qualitative structure of the entire vector field (at least in a qualitative, topological sense) [10]. Thus the configuration of critical point is a powerful tool for the intuitive understanding of the structure. There is only a limited number of qualitatively different critical points. Following the known theory [11, 12, 13],
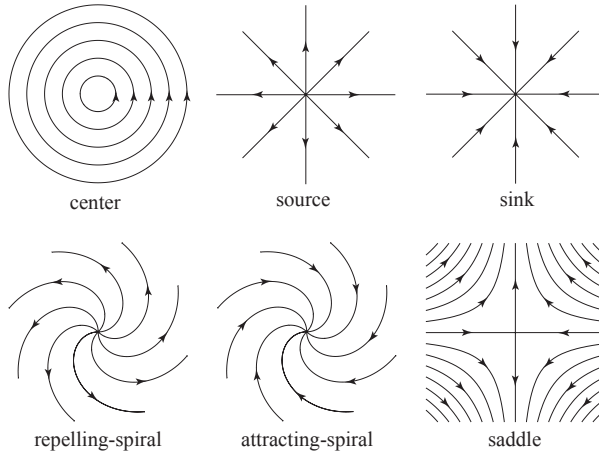
Figure 5.2: Different types of critical points possible in 2D flows

the formal classification of the critical points of a 2D vector field is given by means of eigenvalues of the Jacobian of the vector at the critical point:

$$\frac{\partial(u,v)}{\partial(x,y)}_{x0,y0} = \left[\begin{array}{cc} \frac{\partial u}{\partial x} & \frac{\partial v}{\partial x} \\ \frac{\partial u}{\partial y} & \frac{\partial v}{\partial y} \end{array} \right]_{x0,y0}. \tag{5.3}$$

Figure 5.2 shows all possible critical points of a 2D vector field. On the basis of eigenvalues they can be classified as center $\lambda_1 = \lambda_2$, $i_1 = -i_2$, source $\lambda_1 > 0$, $\lambda_2 > 0$, $i_1 = i_2 = 0$, sink $\lambda_1 < 0$, $\lambda_2 < 0$, $i_1 = i_2 = 0$, repelling focus $\lambda_1 = \lambda_2 > 0$, $i_1 = -i_2 \neq 0$, attracting focus $\lambda_1 = \lambda_2 < 0$, $i_1 = -i_2 \neq 0$ and saddle point $\lambda_1 < 0$, $\lambda_2 > 0$, $i_1 = i_2 = 0$ (where λ_1, λ_2, i_1, i_2 are the real and imaginary parts of the eigenvalues). Unfortunately the terminology is not standard in mathematical theory, here we use terms from [14]. The signs of the real parts of the eigenvalues define the attractive or repelling character and the imaginary parts denote the circulation around the point.

5.4.2 Singular points in the light field

All types of critical points typical for a general 2D vector field occur in the light field. Here we present several simple models illustrating how these critical points can be created and showing the distributions of the flux lines. We assume the light fields to be translationally symmetric (with respect to the axis perpendicular to the plane of the paper) and therefore

the light fields can be represented by planar flux lines in the 2D plane. The flux lines for the models were calculated by means of iterative computer simulations.

The 'source' critical point is the easiest case, it appears for instance in the case of a point light source placed in empty dark space. The flux lines are straight lines radiating from the source. The 'sink' may be found for instance at a small black (light absorbing) sphere placed in Ganzfeld (fully diffuse) illumination. In this case the flux lines are straight lines coming from the Ganzfeld and ending on the surface of the sphere. These two examples of the sink and the source are completely opposite each other and the one can be modified into another by replacing light and darkness. The primary difference is that while the point light source may (if physically possible) be infinitesimally small and of arbitrarily high intensities, the black sphere must be of certain dimension and the amount of light it absorbs is proportional to and thus limited by its surface area. An infinitesimally small black sphere does not not absorb any light and therefore is no sink. There is no such thing as negative radiance, but the effect the black sphere produces on the flux lines in a Ganzfeld is analogous to a negative electrical charge in electrostatic field.

In contrast to the 'source' and 'sink' the saddle point occurs in empty space. Figure 5.3 shows models in which the saddle occurs. In Figure 5.3(a) there are two point light sources of equal intensity. At the point in the middle of them the irradiance is a symmetrical function, so the flux density at that point is zero for all orientations and therefore the light vector vanishes. A similar situation can be constructed by using diffuse area light sources. In Figure 5.3(b) the model consists of two uniformly bright disks opposite to each other, at the point right in the middle between them the light vector is zero and the flux lines form a saddle point.

Figure 5.4(a) shows a model for the 'center' critical point. The model consists of four equal area light sources (indicated by thick lines) located at the periphery of the square, one at each side and separated by gaps of the same size. The shapes of the light sources are infinitely long stripes in the plane orthogonal to the plane of the illustration. We consider the light field in the space enveloped by the square. The space is not occluded and therefore the flux lines should be smooth and continuous. At the periphery the flux lines originate on the light sources and continue their way to the gaps. However, closer to the middle the flux lines are closed, rotating counterclockwise. Right in the middle the light vector vanishes due to the symmetry of the radiance distribution function. The behavior of the flux lines around this critical point clearly indicates that this is a 'center'.

(a)   (b)
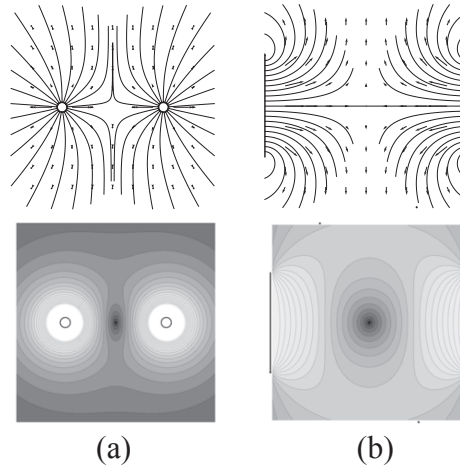
Figure 5.3: Saddle points due to point light sources (left) and diffuse area light sources (right)

Notice that there are also four saddle points, which can easily be found from the contour plots that represent the magnitude of the light vector.

A 'repelling-spiral' critical point can be constructed by adding a point light source in the middle of the previous model (see Figure 5.4(b)). In this case in the center of the space the flux lines originate from the point light source and diverge to the gaps, due the influence of the peripheral light sources the flux lines are twisted into a spirals.

Figure 5.4(c) shows the 'attracting-spiral' critical point. The model consists of the basis model shown in Figure 5.4(a) and a black sphere put in the middle. The light absorbing object in the center works as a 'sink' - it attracts the flux lines from the peripheral light sources. It is important to point out here that an opaque object in a light field occludes light, therefore there are areas where individual light sources are completely occluded (notice the little black star in the middle of the contour plot). The screening effect causes discontinuities of the flux lines, however this problem occurs only in a small area very close to the sphere.

(a)　　　　　　　　(b)　　　　　　　　(c)
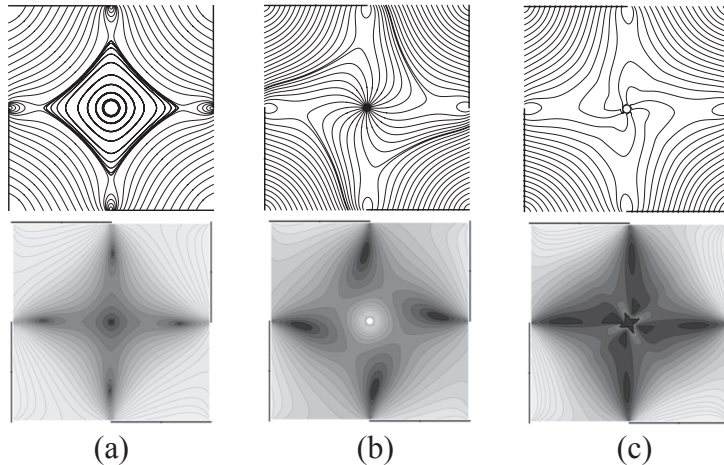
Figure 5.4: Examples of a center (left), repelling-spiral (point light source in the middle) and attractive spiral (black sphere in the middle) critical points.

5.5　Discussion and conclusions

In this article we analyzed topological aspects of light fields. We have shown that all generic topological structures typical for 2D vector fields may also occur in light fields and illustrated the possible configurations by modeling. The models provide intuitive and simple examples of what kind of qualitative structures may occur. In order to describe the qualitative structure of the light field we don't have to know the light vector at all points of space, but instead it may be given merely by pointing out the singular points and describing the behavior of the flux lines in their vicinity. We considered only 2D cases for simplicity, but in a similar way the analysis can be extended to 3D.

　　Considering the light field as a vector field gives us a description of radiant flux transfer through space, which may be used for practical purposes in architecture, interior design, etc. In fact photographers and designers do simple manipulations with the flux in order to achieve the desirable effects by placing black and white sheets (e.g. screens or umbrellas) next to the illuminated object.

　　The light vector gives a very rough approximation (only first order) of the radiance

distribution function, nevertheless it contains information which is important for object appearance since the projection of the light vector on a surface gives the irradiance. The light field depends not only on the primary light sources. The contribution of light scattered from the objects is also important. For instance flux lines would bend around (without touching) a white sphere placed into diffuse illumination and would end on a black object. Knowing the structure of the light field one can predict the shading patterns of objects in a scene and one can manipulate the structure of the light field by putting additional objects into the scene (screens, photographer's umbrella). Optical interactions between light fields and objects in it are of special importance because it is directly related to applications. Computer graphics algorithms frequently sacrifice physical laws and precision in order to achieve greater speed. However only physically based approaches [6] can be correct.

The screening effect does not allow to develop a general theory of the light field in terms of differential equations, but for unoccluded areas this can be done [2]. It would be interesting to consider special cases of light fields such as, for instance, 'center' critical point.

In order to make the illustrations as intuitive as possible the models which we constructed in this article were constructed in the most simple way by considering 'point light sources' and uniformly diffuse area light sources. However more complicated models could be constructed by means of nonuniform light sources.

We believe that understanding the singular points of light fields provides fundamental insights into the global structure of natural light fields. This approach can be used in practice for the needs of lighting engineers. Singular points of light fields in a region of space can be found in practice by measuring light vectors and analyzing the behavior of flux tubes in that region.

BIBLIOGRAPHY

[1] A. Gershun, 'The light field,' J. Math. Phys. **18**, 51-151. (1939) (translated by P. Moon and G. Timoshenko).

[2] P. Moon, D. E. Spencer, *The Photic Field*, (MIT Press, 1981).

[3] E. H. Adelson and J. Bergen, 'The plenoptic function and the elements of early vision,' in *Computational Models of Visual Processing*, M. Landy, and J. Movshon, eds. (MIT Press, 1991), pp. 3-20.

[4] G. Greger, P. Shirley, P. Hubbard, and D. Greenberg, 'The irradiance volume,' *IEEE Computer Graphics & Applications*, **18(2)**, 32-43 (1998).

[5] J. Arvo, 'The Irradiance Jacobian for Partially Occluded Polyhedral Surfaces,' in *Computer Graphics Proceedings*, 1994, pp. 343-350.

[6] J.J. Koenderink, A.J. van Doorn, 'Shape and shading,' In: *The visual neurosciences*, L.M. Chalupa, J.S. Werner (eds.), MIT Press, Cambridge, pp. 1090-1105, (2003).

[7] Mury A.A., Pont S.C., Koenderink J.J., 'Representing the Light Field in Finite 3D Spaces from Sparse Discrete Samples,' submitted to Applied Optics, 2008.

[8] D.V. Bakharev, 'About the structure of light fields,' Svototekhnika, **3**, pp. 40-44, (2005) *in Russian*.

[9] http://www.megatron.co.uk/cim/index.html

[10] J. C. Maxwell, 'On hills and dales,' Philosophical Magazine **40**, 421-427(1870).

[11] M. Tabor, 'Classification of fixed points,' 1.4.b in *Chaos and Integrability in Nonlinear Dynamics: An Introduction*, (New York, Wiley, 1989).

[12] M.S. Chong, A.E. Perry, B.J. Cantwell, 'A general classification of three-dimensional flowfields,' Physics of fluids A, **2(5)**, pp. 765-777, (1990).

[13] M. Tobak, D.J. Peake, 'Topology of three-dimensional separated flows,' Annual review of fluid mechanics, **65**, pp. 61-85, (1982).

[14] J. L. Helman, Lambertus Hesselink, 'Surface representations of two and three-dimensional topology,' IEEE Computer Graphics and Applications, **11(3)**, 36-46(2000).

[15] C. Cuttle, 'Cubic illumination,' Lighting Research and Technology, **29(1)**, pp. 1-14, (1997).

[16] V. Verma, D. Kao, A. Pang, 'A Flow-Guided Streamlines Seeding Strategy,' *Proc. IEEE Visualization*, (2000), pp. 163-170.

[17] C. Cuttle, 'Lighting Patterns and the Flow of Light,' Lighting Research and Technology **3(3)**, 171-189(1971).

Appendix.
On visualization of light fields

The 'quality of light' for a long time used to be a term from the lexicon of artists. For instance painters, designers and architects used to describe illumination conditions in poetic terms such as light 'creeping around' and 'washing' objects, 'oceans of light' and so on. Which indeed makes the language of artists beautiful and poetic, but nevertheless ambiguous and difficult to understand for engineers. The applications in illumination engineering, architecture and interior design require formal, technical descriptions of the quality of light in terms of quantifiable parameters. Such descriptions should also be meaningful. In this Appendix we summarize existing techniques for the visualization of light fields, give additional examples which illustrate the usefulness of the results presented in this thesis and also describe methods which have not been shown in previous chapters.

For a local light field, which is essentially a spherical function describing the radiance distribution at a point in three-dimensional space, the most important qualitative properties for an object's appearance are the primary direction of light and degree of diffuseness. In this way one can define three so called 'canonical' cases of light fields: collimated illumination (like direct sunlight), hemispherically diffuse illumination (for instance an overcast sky) and Ganzfeld illumination (uniformly diffuse illumination such as a polar white out). Collimated and Ganzfeld cases are completely opposite to each other in terms of diffuseness, one being extremely directional (point light source at infinity, in the terminology of computer graphics) and the other absolutely diffuse (ambient light in computer graphics). Hemispherically diffuse illumination is an intermediate condition
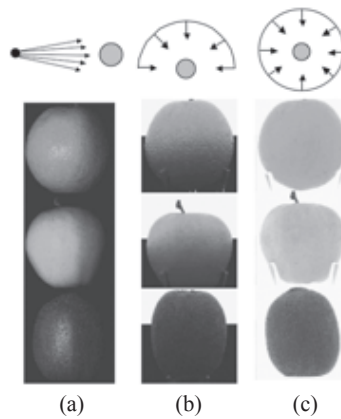
Figure A-1: Top row shows the schematics of three canonical cases of light field: collimated (left), hemispherically diffuse (middle) and Ganzfeld (right) illuminations. The photographs of simple convex objects (orange, apple and kiwi) demonstrate different form revealing effects of light.

and possesses properties of both extreme cases - it is diffuse but at the same time directional (directionally diffuse). Figure A-1 shows the schematics of canonical light fields and photographs of different objects in these cases. Notice that these light fields produce qualitatively different effects on object appearance. For instance, collimated light reveals the texture very well due to strong contrast between lit and unlit areas. In this case there is all-or-none vignetting but no partial occlusion of the light source. In the case of a hemispherically diffuse source the vignetting is gradual. In the case of Ganzfeld illumination the form revealing effect is only due to vignetting and therefore convex Lambertian objects of a uniform smooth material would appear flat.

The diffuseness of light is not restricted to three canonical cases. In order to describe the diffuseness of illumination Frandsen ('The scale of light', 1987) introduced the notion of the 'scale of light'. He varied the size of a spherical aperture from narrow ($1°$, almost collimated) to hemispherically diffuse ($180°$) in a systematic way such that the illumination incident on a horizontal plane varied exponentially. Figure A-2 shows the 11 scales of light according to Frandsen. Thus, the degree of diffuseness can be approached in a formal way. Figure A-3 shows how an object's appearance changes as we vary the diffuseness of light by changing the size of the aperture from $90°$ to $270°$.

(a)	(b)
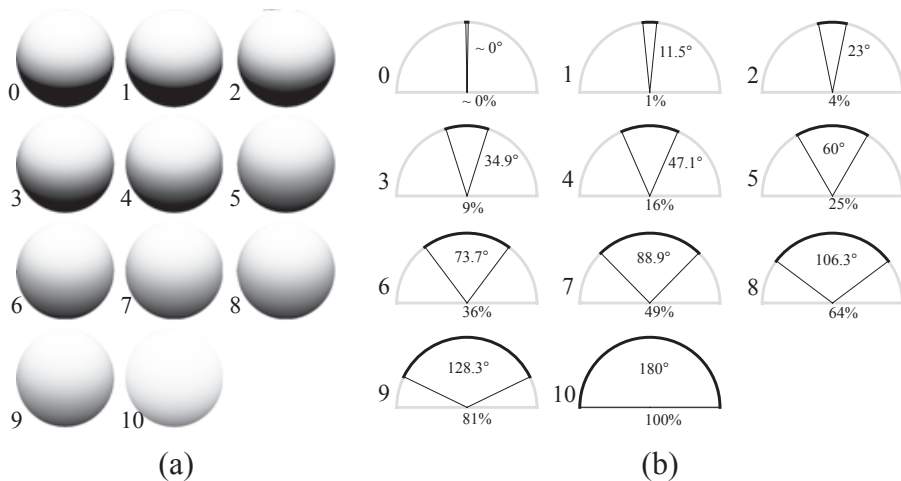
Figure A-2: The scale of light (Frandsen, 1987). Changing the size of the aperture through which the light comes from 1 to 180 degrees, one can achieve qualitatively different shadings varying from sharp (in the case of collimated light) to smooth (hemispherically diffuse). The schematics on the right show the apertures for 11 scales of light, the picture on the left shows the shading variations over the surface of a sphere for those scales of light.

In general the light field is a rather complicated function and usually it cannot be described only by giving the primary direction of the light and its diffuseness. In some cases there is no primary direction, or there are more than one light source and light comes from multiple directions with similar intensities and therefore all directions should be considered. For instance Figure A-4 shows a head illuminated from above by a directed light source, however there is a white screen under the object and diffuse light reflected by the screen illuminates the object from below. The contribution of the upper lobe is stronger, however the diffuse lower lobe cannot be ignored - the effects are clearly visible at the object. More complex cases can be constructed easily.

Properties of the light field are easily defined theoretically, but rather difficult to estimate empirically. For instance, there is no measurement device that can estimate the scale of light. Some characteristics of light can be revealed from the appearance of objects. Architects and interior designers typically use special reference objects for that purpose.
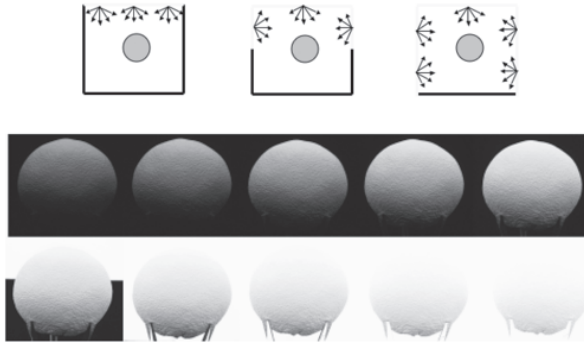
Figure A-3: Diffuseness variation. Photographs of an object (a Lambertian sphere with rough texture) in light fields of different diffuseness. The size of the aperture varies from 90° to 270° in equal steps of 20°, the schematics show the 90°, 180° and 270° cases.

Figure A-4: A light clamp. The head is illuminated from above by a directed light source and light scattered by a white screen illuminates the head from below. Light comes to the object from two opposite directions resulting in a 'clamp'.

For instance from an image of a white sphere the direction of the flow of light can be judged, and from the shading gradient over the surface of the sphere the diffuseness of illumination can be inferred. In the case of collimated light the border that separates lit and unlit areas is very sharp and clear, while in the case of diffuse illumination the termi-

nator is smoothed out. Carrying an object over a scene one can judge from its appearance how illumination changes over the scene. Cuttle ('Lighting by design', 2003) suggested to use three reference objects to reveal different aspects of light fields - a white matte sphere, a shiny black sphere and a white disk with a stem. These three objects were chosen to assess different lighting effects. According to Cuttle, the white sphere indicated the primary direction of light, the shiny black sphere revealed the primary light sources which are clearly visible in the image of the black sphere as highlights, and the 'peg-on-a-disc' object revealed the shadow quality (the peg casts shadows on the disc, and from the sharpness of cast shadows the diffuseness of illumination can be judged). These reference objects are useful for making quick intuitive estimations of the quality of the light. However, in some illumination conditions the images of reference objects are ambiguous. For instance, in diffuse illumination the white sphere appears almost uniformly bright since the shading gradient is not strong. Furthermore, psychophysical research has shown that simultaneous judgments of illumination direction and diffuseness from the appearance of a matte white sphere interact with each other. So, the conclusions made on the basis of these objects are very subjective.

We developed several other models of light probes. Figure A-5 shows Radiance renderings of three models: a polyhedron (subdivided icosahedron) (a), a 'bubbled sphere' (b) and a cube with radial patterns of corrugations on its sides (c). We rendered these objects in Frandsen's 11 scales of light (from collimated to hemispherically diffuse) and in Ganzfeld illumination in order to demonstrate that these objects might be useful additions to describe properties of diffuse light. For instance, it is easier to visually judge the shading pattern from a faceted surface with distinct brightnesses than from a smooth white sphere where the shading gradient is smooth. The 'bubbled sphere' provides information about the light field on two levels - a global (overall object) and a local level. The cube helps to estimate the light direction. It is easy to judge which sides of the ridges on the cube's sides are brighter and thus infer the primary illumination direction even in diffuse illumination (except for Ganzfeld, of course).

Figure A-6 shows real probes that we developed and used to probe diffuse light fields. The bubbled sphere is similar to the model. The sphere, the icosahedron (20 faces, lower right object) and dodecahedron (12 faces, lower center object) reveal that the light is coming from the upper left quadrant, and that it is directionally diffuse. These objects reveal the quality of light in a more salient way than a matte white sphere due to the meso-scale 'texture' and non-smooth shading gradients. Knowing the orientation of the facets and

their luminance the illumination distribution solid at that point could be reconstructed. The concave icosahedron (lower left object) has 60 internal facets (which are affected by inter-reflections) and 20 outer 'facets'. The cast shadows in the concavities allow for an even more accurate judgment of the illumination direction. However, a single photograph of a matte light probe cannot completely describe the local light field (a spherical radiance distribution function). Several photographs from different viewing points would be needed to describe the local light field. Therefore, although these reference objects are useful for quick semi-quantitative estimates of the lighting conditions and may replenish the toolkit of architects and interior designers, they are not very suitable for formal scientific measurements.

Common techniques to capture an entire radiance distribution function at a point are panoramic imaging or photography of a mirror sphere which reflects light incident from all directions. Another possibility is to use more advanced light measuring devices. Our custom-made light measuring device Plenopter is capable of measuring local light fields up to the second order (9 basis functions) in terms of spherical harmonics (see *Chapter 2* for details). Basically we get 9 coefficients which are the shape descriptors (the device and the procedure are described in *Chapter 3*). The coefficient values are not very informative in themselves, so a visualization method is needed. The nature of spherical harmonics allows us to represent the first order contribution as a vector, and the second order contribution (which is a symmetry function with axes of symmetry orthogonal to each other) as two orthogonal vectors describing its positive and negative components. The first order component is the light vector which describes the primary direction of radiant flux. The second order term is the quadruple (or 'squash tensor') which can capture a wide variety of shapes from a 'clamp' to a 'ring' (see *Chapter 2*). Figure A-7 shows the results of two Plenopter measurements in the same scene but in different illumination conditions - under an overcast sky (the upper one) and in direct sunlight (lower one). The fish-eye lense photographs of sky and ground (left side of the figure) provide a description of the environment. Notice that in the case of diffuse overcast illumination there is primarily one direction of light - from above. However in the case of direct sunlight there is also strong scattering from the ground. These details are clearly shown by the measurements: in the overcast sky case the structure of the light field is dominated by the light vector, while in the direct sun-light condition the squash tensor dominates, indicating a 'light clamp'.

Other examples of Plenopter measurements are shown in Figure A-8. We considered a room scene in four different illumination conditions (see *Chapter 4* for details). The
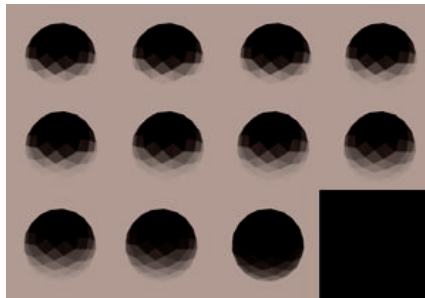
(a)
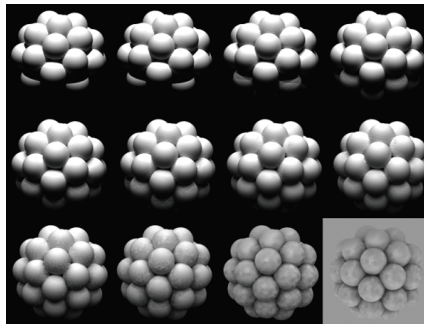
(b)
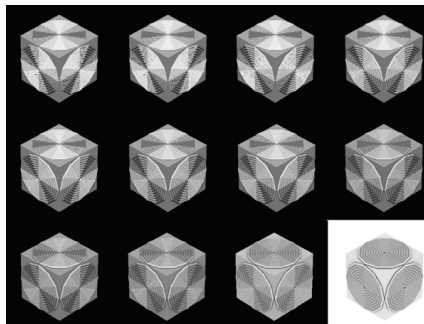
(c)

Figure A-5: Radiance renderings of the models of light probes for diffuse light. A polyhedron (a), a bubbled sphere (b) and a cube with radial patterns of corrugations on its sides (c) rendered in Frandsen's 11 scales of light and in Ganzfeld illumination (low right).
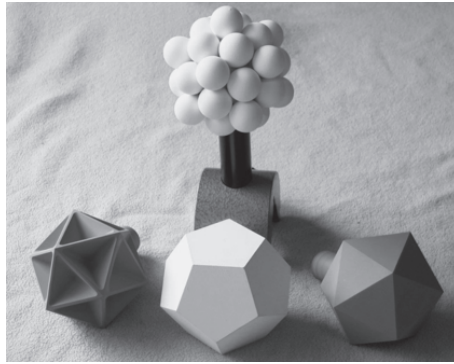
Figure A-6: Real light probes which we used for estimating the quality of diffuse light fields. A bubbled sphere, icosahedron, dodecahedron and concave icosahedron (upper, right, lower middle and left objects).

measurements were taken in the center of the room, the illumination conditions were the following: diffuse light from the upper-left (a), a diffuse circular area light source in the center of the ceiling right above the measurement point (b), four strongly directed light sources in the corners of the ceiling pointing downwards (c), three area light sources positioned in chess-order on the ceiling (d). The upper row in Figure A-8 shows the photographs of mirror balls positioned at the measurements points. The geometry of the scene and the distributions of the light sources are clearly visible on these images. The second row shows the vector representations of the Plenopter measurements. Notice that the vector representations correspond very well to the scenes. In case (a) the light vector and the positive part of the squash tensor are oriented in the direction of the upper-left wall, where the light comes from. In case (b) the light vector and the squash tensor are aligned together almost vertically pointing at the circular area light source on the ceiling. In case (c) the primary light sources are close to collimated and their beams don't extend to the center of the room, where the measurements were taken. The strongest component of the light field at the center of the room in this case is due to scattering from the ground and therefore the light field should be very diffuse at that point. The illumination direction is indicated by the light vector which is pointing downwards, clearly showing that indeed the strongest contribution to the light field at that point is due to scattering from the floor. In case (d) the light vector and squash tensor point towards the closest of the three sources. The third row shows the shape of the approximation of the spherical radiance distribution.
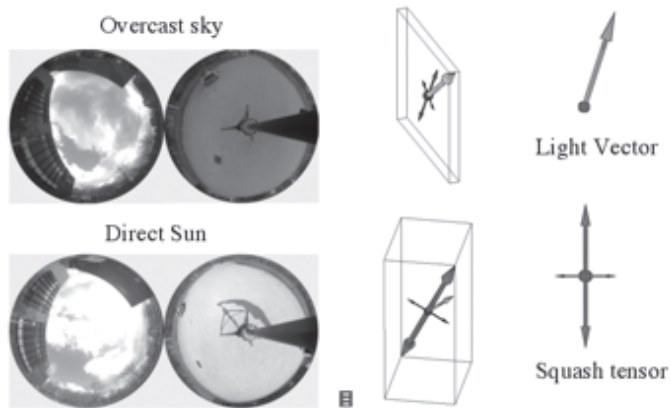
Figure A-7: An example of Plenopter measurements, for overcast versus direct sunlight conditions. On the left we show fish-eye lense photographs of the sky and ground which describe the scenes. On the right the vector representations of Plenopter measurements are shown. The upper row describes the overcast sky condition, the lower row shows the same scene in direct sun light. Notice that in the case of direct sunlight there is strong scattering from the ground and therefore the squash tensor dominates in the structure of the light field.

Notice that in case (c) the radiance distribution function is very diffuse (roughly spherical) as expected. The lowest row shows the contour plots which represent the second order light fields projected to a plain.

The methods we described so far are suitable for estimation and visualization of local light fields. However it is frequently needed to assess light fields of entire three-dimensional scenes. This can be done semi-quantitatively by, for instance, carrying light probes around the scene and taking photographs of the light probes at certain grid points over the scene (the so-called 'light-flow-meter' approach). For quantitative measurements we can take Plenopter samples at points of a regular grid of the scene. Figure A-9(a) shows 15 Plenopter measurements over a regular grid in the scene described in Figure A-8 (d), with three area light sources on the ceiling positioned in chess-order. It is difficult to judge the global light field's structure from such a representation, except for the fact that at points 3, 7 and 15 (the points which are closest to the light sources) the illumination is stronger. A better visualization of the global structure could be provided by contin-

(a) (b) (c) (d)
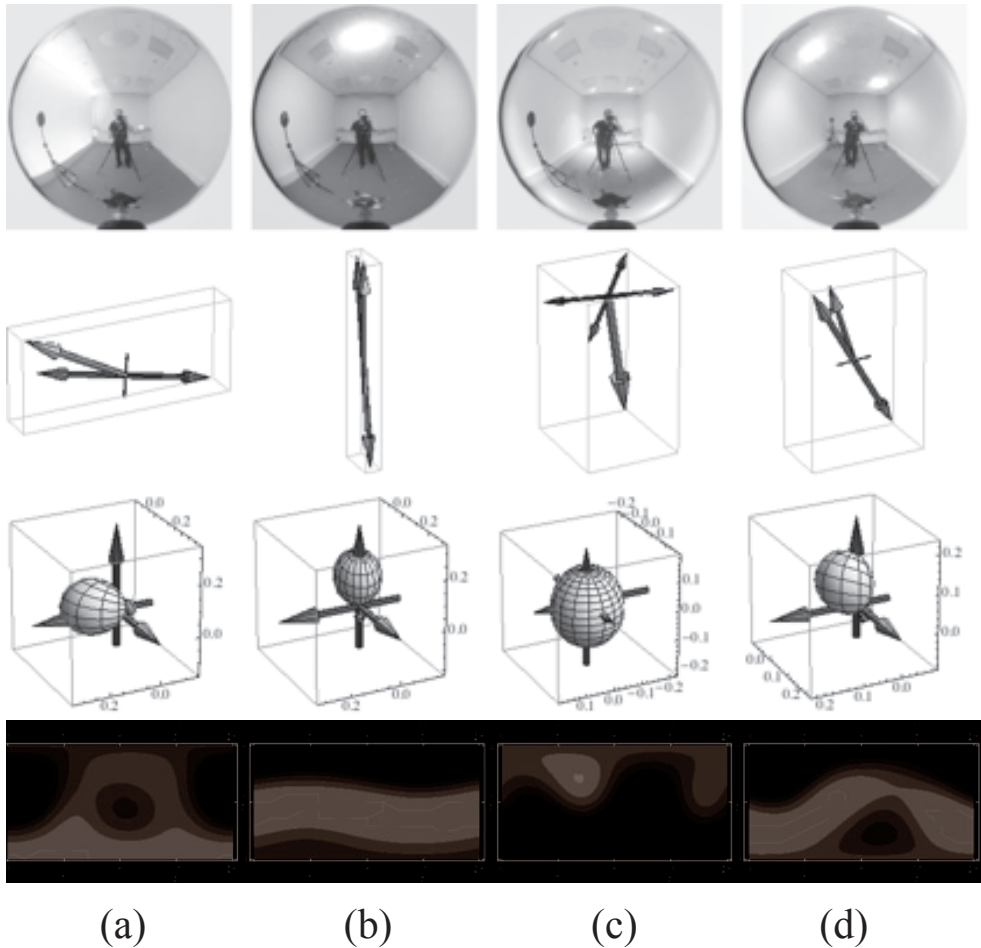
Figure A-8: Visualization of Plenopter measurements. The upper row shows photographs of a mirror ball placed at the measurements points. The second row shows vector representations of Plenopter measurements. The third row shows spherical radiance distribution functions smoothed out to the second order spherical harmonic approximation. The lower row shows contour plots which represent the second order light fields projected to a plain.

uous data achieved by interpolation. Figures 9(b1, c, d) show the contour plots which represent the magnitudes of the light vector, zero order component and squash tensor correspondingly over the measurements plain. The contour plots were calculated by means of interpolation on the basis of 15 measurements. Figure A-9(b,2) shows the projection of the light vectors into the measurement plain. The light vectors clearly point in the directions of the light sources. However, this kind of visualization is ambiguous in itself, while a combination of three planar projections is very hard to integrate, and therefore not very practical. We need a technique which provides a meaningful representation of these three components in three-dimensional space.

Since we can calculate the light vector at any point of the scene, the light field can be considered as a vector field and therefore we can use existing techniques for vector field visualizations. Gershun ('The light field', 1936) suggested to use tangential curves (flux lines) for visualization of the light field. Figure A-10 shows some of Gerhsun's drawings of light fields by means of flux lines and light tubes. At that time it was rather difficult to calculate or measure the flux lines and therefore some of the drawings were made merely by intuition. For instance, as it was pointed out by Bakharev (D.V. Bakharev, 'About the structure of light fields', Svetotekhnika, 2005) the flux lines in Figure A-10(d) cannot be continuous and accurate modeling may prove that.

Nowadays we can calculate precisely the flux lines, visualize the distribution of the radiant flux by means of light tubes, and even measure those descriptors in real three-dimensional scenes (see *Chapter 4* for details). The light tubes provide a very intuitive visualization of the flux propagation through the scene and describe the quality of light very well. In Figure A-11(a) we show the flux tubes distribution for a room scene with only one light source - a circular diffuse area light source on the ceiling (the model is based on the scene showed in Figure A-8(b)). The light tubes typically originate at the light sources and end on light absorbing surfaces diverging radially from the middle of the ceiling as is shown in close-up in figure A-11(b). In figures 11 (c) and (d) we inserted Lambertian black and white spheres right under the source. Notice how the light tubes bend around the spheres - in the case of the black sphere (c) the tubes bend over it and end up on the lower part of the sphere because it absorbs light, while the white sphere reflects light and works as a secondary light source pushing off the light tubes. Indeed the tubes 'creep over' the sphere, and thus this visualization is an example of how our method may clarify the poetic language of artists for engineers. As we showed on Figure A-11 the global structure of the light field can be studied and visualized by means of the light

(b,1)   (b,2)

(a)   (c)   (d)
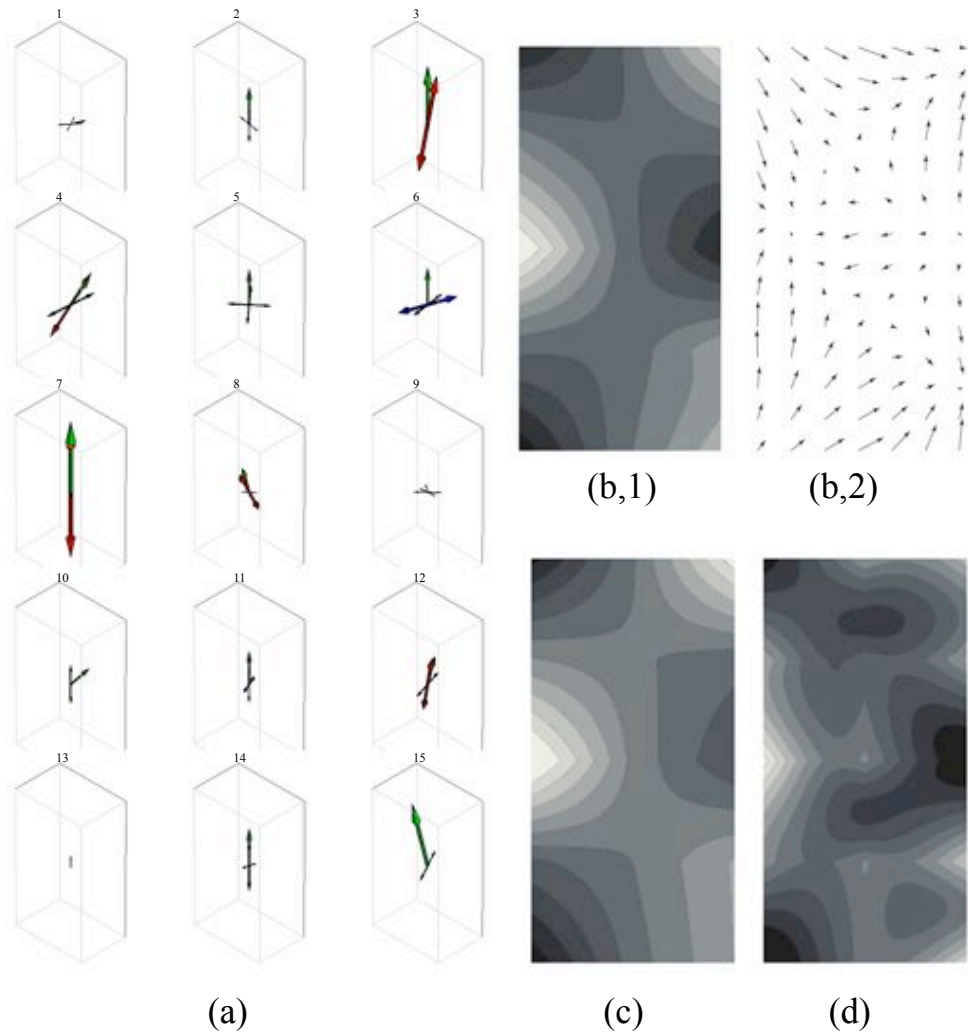
Figure A-9: Plenopter measurements over an array of points; (a) Plenopter measurements over a regular grid of the scene which is shown in Figure A-8(d); b1, c, d show contour plots which represent the strengths of the light vector (b), zero order component (c) and squash tensor (d); b2 shows a projection of the light vectors into the measurements plain (see text for details).

(a) (b) (c)

(d) (e) (f)
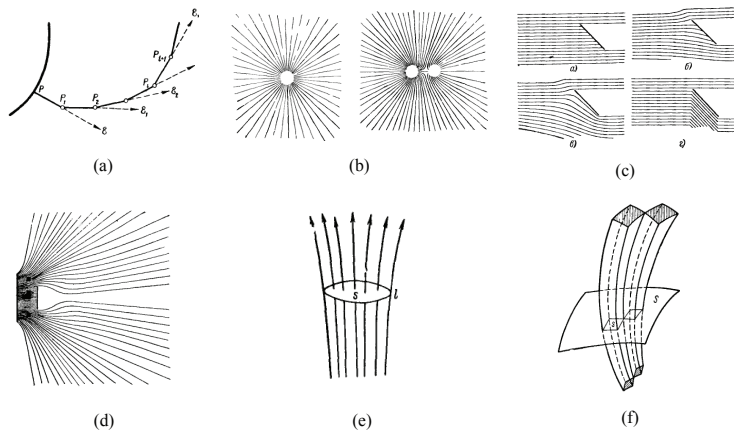
Figure A-10: Gershun's drawings on light field visualization; (a) iterative drawing of flux lines by calculating the light vector from point to point in small steps; (b) flux lines due to a point light source (left) and a 'dipole' due to two light sources next to each other (right); (c) slanted Lambertian screen in collimated light, the albedo of the screen changes from 0 (black screen) to 1 (notice how the flux lines bent over the screen in the last image); (d) a light field due to a uniform luminous disc with a screen in front of it (the flux lines bent over the screen); (e), (f) drawings of light tubes. These images were taken from the Russian version of Gershun's book ('Svetovoe pole', 1936) and do not appear in the translated version.

tubes. We believe that these visualization and measurement techniques might be useful for wide variety of applications.

The light field influences the appearance of objects. Conversely, the addition of objects in a scene influences the light field. The example with black and white spheres inserted into the light field shows how optical interactions between the light field and objects in it can be understood intuitively. Typically the problem of interaction between light and the scene is left to hard core computer graphics. However, as we have shown, if we aim for low order, visually relevant, insightful representations this problem can be simplified a lot. Describing how light fields interact with objects in scenes in a quantitative though intuitive way is a challenging topic for future research.

(a)

(b)   (c)   (d)
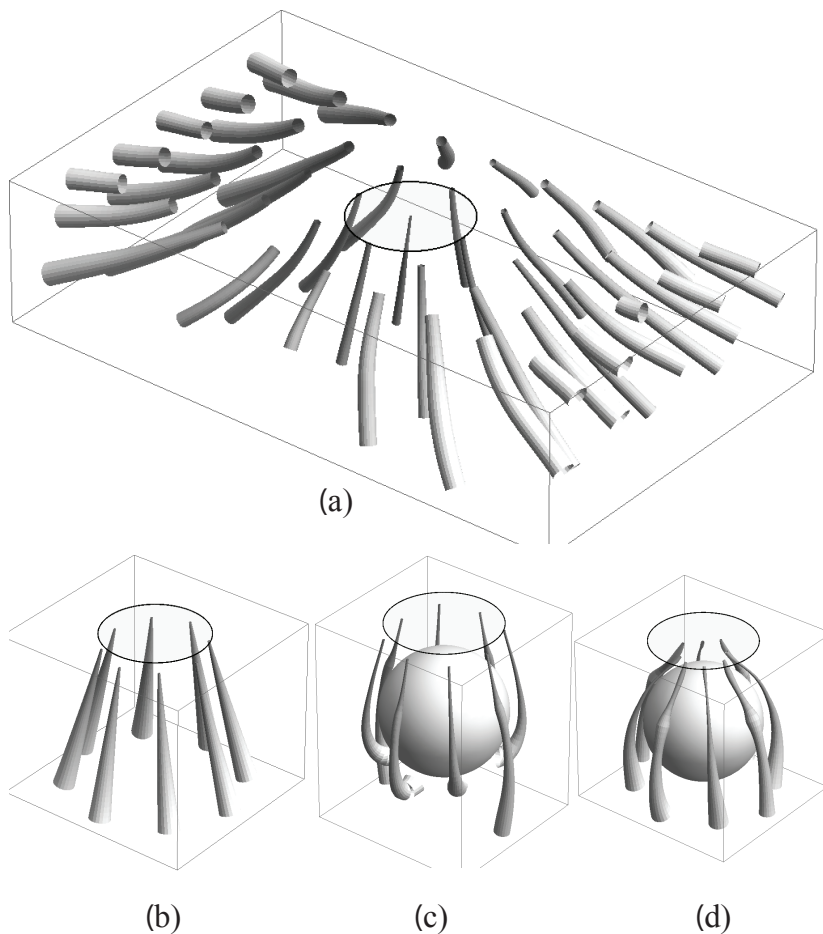
Figure A-11: Example of interaction between the light field and the objects in the scene. The model is based on the scene shown in Figure A-8(b), a room with a circular area light source in the center of the ceiling. (a) the light tubes show the transport of radiant flux over the scene (notice how the light tubes diverge radially from the light source); (b) shows a close-up of the center point of the light field; (c) a black sphere is put right under the light source, notice that the light tubes end up on the surface of the light absorbing black sphere; (d) a white sphere is put into the scene, the light tubes bent around it since the reflected light 'pushes' them away.

SUMMARY

This thesis focuses on the properties of light fields with respect to object appearance. More specifically, our interest was mainly directed to the structure and spatial variation of light fields in natural scenes. We approached the structure of light fields by means of spherical harmonics which allows one to divide the complicated spherical functions of local light fields in frequency bands and to analyze those separately. In *chapter 2* we empirically studied the variation of different frequencies of light field approximations over natural scenes by means of panoramic photography and found that the low order components show systematic and stable spatial variations whereas the high order components vary rapidly and chaotically over most scenes. We showed how the 'quality of light' can be expressed by means of a light vector and a squash tensor which provide a formal mathematical but nevertheless very intuitive way of representation bridging the gap between scientific and artistic understandings of light. In *chapter 3* we continued the study of the spatial behavior of light fields more thoroughly considering complicated scenes and focusing on the 2nd order structures which we measured by our custom made device. In *Chapter 4* we presented a technique with which the 2nd order descriptions can be recovered for an entire three dimensional scene on the basis of a limited number of measurements and presented a visualization of the structure of light fields by means of light tubes. *Chapter 5* was devoted to possible topological structures of light fields. In the *Appendix* we provided additional examples of methods, measurements and visualization of light fields.

In *chapter 2* we considered simple scenes such as typical 'street', 'wall' and 'forest' scenes and studied the spatial variation of light fields along the main axes of symmetry of the scenes. The measurements were performed photographically by utilizing panoramic imaging. We described the local light fields in terms of spherical harmonics up to the $10th$ order and analyzed the qualitative properties and physical meanings of the low order components. We took a first step in a further development of Gershun's classical work

on the light field by extending his description beyond the three-dimensional vector field, towards a more complete description of the light field using tensors. We showed that the three first components, namely the monopole (density of light), the dipole (light vector) and the quadrupole, which we named 'squash tensor', suffice to describe a wide range of qualitatively different light fields. The empirical analysis allowed us to conclude that the low order components dominate the structure of most light fields. The low order components are rather constant over the scenes whereas high order components are not. Using simple models, we found a strong relation between the low order components and the geometrical layouts of the scenes.

In *chapter 3* we presented a new technique to capture the global structure of the light field in terms of spherical harmonics functions. Our custom made device Plenopter allows to perform measurements of light fields up to the second order easily, quickly and with a high dynamic range. Using that device we continued the research presented in *chapter 2* by considering measurements across the scenes, along the line orthogonal to the main axis of geometrical symmetry. The measurements clearly indicate that in scenes of similar geometry the light fields demonstrate characteristic variations of the light vector and the squash tensor over the scene. This happened despite the fact that the scenes possessed different reflective properties and even were differently oriented with regard to the primary light sources.

In *chapter 4* we presented a method for measuring, reconstructing and visualizing the global structures of light fields in finite 3D spaces. We used the Plenopter to measure second order light fields at points over a regular grid and interpolate the spherical harmonics coefficients to calculate the light fields at all points of a closed 3D space.

We presented a new way of visualizing the light field in 3D space by means of light tubes which indicate the radiant flux transfer and provide intuitive insights into the global structure of the light field through the entire space of the scene.

In *chapter 5* we considered possible topological structures of light fields. We studied singular points and showed that all generic topological structures that are possible for 2D vector fields may also occur in the case of light fields. We provided models which showed that light tubes can even be closed. The global structure of the light field may be described by means of the singular points.

Samenvatting

Dit proefschrift richt zich op de eigenschappen van lichtvelden in relatie tot de visuele verschijningsvorm van objecten. Onze aandacht ging hierbij specifiek uit naar de structuur en spatiele variatie van lichtvelden in natuurlijke scenes. We hebben de structuur van lichtvelden benaderd door middel van bolfunkties, die het mogelijk maken de gecompliceerde sferische funkties van lokale lichtvelden onder te verdelen in frequentiebanden en die separaat te analyseren. In *hoofdstuk 2* hebben we de variatie van verschillende frequenties van lichtveld-benaderingen over natuurlijke scenes empirisch bestudeerd door middel van panoramische fotografie en vonden dat de lage orde componenten systematische en stabiele variaties lieten zien, terwijl de hoge orde componenten snel en chaotisch variëren over de meeste scenes. We hebben laten zien hoe de 'kwaliteit van licht' uitgedrukt kan worden door middel van een lichtvector en een squash tensor, wat een formele mathematische, maar desondanks zeer intuitieve representatie biedt die het gat tussen het wetenschappelijke en artistieke begrip van licht overbrugt. In *hoofdstuk 3* hebben we onze studie naar het spatiele gedrag van lichtvelden voortgezet door gecompliceerde scenes te beschouwen en te focussen op de 2*de* orde structuren die we hebben gemeten met ons zelf-ontworpen apparaat. In *hoofdstuk 4* presenteerden we de techniek waarmee op basis van een beperkt aantal metingen de 2*de* orde beschrijvingen geconstrueerd kunnen worden voor een gehele drie-dimensionale scene en presenteerden we een visualisatie van de structuur van lichtvelden door middel van lichtbuizen. *Hoofdstuk 5* was gewijd aan mogelijke topologische structuren van lichtvelden. In de *appendix* hebben we additionele voorbeelden gegeven van methodes, metingen en visualisaties van lichtvelden.

In *hoofdstuk 2* beschouwden we simpele scenes zoals typische 'straat', 'muur' en 'bos' scenes en bestudeerden de spatiele variatie van lichtvelden langs de hoofd-symmetrie-as van die scenes. De metingen werden fotografisch gedaan door gebruik te maken van panoramische beeldvorming. We beschreven de lokale lichtvelden in termen van bolfunkties tot en met de 10*de* orde en analyseerden de kwalitatieve eigenschappen en fysische

betekenissen van de lage orde eigenschappen. We namen een eerste stap naar een verdere ontwikkeling van Gershun's klassieke werk over het lichtveld door zijn beschrijving als een driedimensionaal vector veld uit te breiden en meer compleet te maken met tensoren. We lieten zien dat de eerste drie componenten, namelijk de monopool (lichtdichtheid), de dipool (lichtvector) en de quadrapool, die we de 'squash tensor' hebben genoemd, voldoen om een groot bereik van kwalitatief verschillende lichtvelden te beschrijven. Uit de empirische analyse konden we concluderen dat de lage orde componenten de structuur van de meeste lichtvelden domineren. De lage orde componenten zijn relatief constant over de scenes, terwijl de hoge orde componenten dat niet zijn. Met gebruikmaking van simpele modellen vonden we een sterke relatie tussen de lage orde componenten en de geometrische layout van de scenes.

In *hoofdstuk 3* presenteerden we een nieuwe techniek om de globale structuur van het lichtveld te vangen in termen van bolfunkties. Met ons zelfgemaakte apparaat Plenopter kunnen we makkelijk, snel en met hoog dynamisch bereik metingen doen van lichtvelden tot en met de tweede orde. Met dit apparaat hebben we ons onderzoek uit *hoofdstuk 2* voortgezet door metingen te beschouwen overlangs scenes, langs de lijn loodrecht op de hoofd-symmetrie-as. De metingen laten duidelijk zien dat in scenes met een gelijksoortige geometrie de lichtvelden karakteristieke variaties over de scene tonen van de lichtvector en squash tensor. Dit resulteerde ondanks het feit dat de scenes verschillende reflectantie-eigenschappen hebben en zelfs verschillend georienteerd waren ten opzichte van de primaire lichtbronnen.

In *hoofdstuk 4* presenteerden we een methode om de globale structuur van lichtvelden in eindige 3D ruimtes te meten, reconstrueren en visualiseren. We gebruikten de plenopter om tweede orde lichtvelden te meten op punten van een regelmatig rooster en interpoleerden de bolfunktie coefficienten om de lichtvelden op alle punten van een gesloten 3D ruimte te berekenen. We presenteerden een nieuwe manier om het lichtveld in een 3D ruimte te visualiseren door middel van lichtbuizen, via welke het stralingsvermogen zich door de ruimte verspreidt en intuitieve inzichten geven in de globale structuur van het lichtveld door de gehele ruimte van de scene.

In *hoofdstuk 5* beschouwden we mogelijke topologische structuren van lichtvelden. We bestudeerden singuliere punten en lieten zien dat alle generieke topologische structuren die mogelijk zijn voor 2D vectorvelden ook kunnen voorkomen als lichtvelden. We gaven modellen die demonstreerden dat lichtbuizen zelfs gesloten kunnen zijn. De globale structuur van het lichtveld kan beschreven worden door middel van de singuliere

punten.

PUBLICATIONS

Mury A.A., Pont S.C., Koenderink J.J.: Spatial properties of light fields in natural scenes. In: Proceedings APGV 2007, ACM SIGGRAPH, Spencer S.N. (Ed.), 140, 2007.

Mury A.A., Pont S.C., Koenderink J.J.: Light field constancy within natural scenes. Applied Optics, 46(29), 7308-7316, 2007.

Mury A.A., Pont S.C., Koenderink J.J.: Analysis of second order light fields in closed 3D spaces. In: Proceedings Frontiers in Optics 2008, OSA, Illumination Modeling Workshop, 2008.

Mury A.A., Pont S.C., Koenderink J.J.: Representing the Light Field in Finite 3D Spaces from Sparse Discrete Samples, submitted to Applied Optics.

Mury A.A., Pont S.C., Koenderink J.J.: The structure of light fields in natural scenes, submitted to Applied Optics.

Mury A.A., Pont S.C., Koenderink J.J.: Topological structures of light fields, submitted to JOSA A.

CURRICULUM VITAE

Alexander Alexeevich Muryy was born in Khabarovsk (Russia) on the 9th of November 1981. After graduation from high school he went to the Far Eastern State Transportation University (FESTU) in Khabarovsk where he studied Applied Mathematics. As a student he pursued research in the area of Optics and studied light propagation in nonlinear crystals. After graduation cum-laude in 2003 he started working as a research assistant in the Optics department and as a junior teacher at the Applied Mathematics department in FESTU. In the end of 2003 he went to do an internship at Groningen University (the Netherlands) where he studied educational processes and logistics for 5 months. In July 2004 he got an appointment as a PhD student at the Ecological Optics group at Utrecht University under supervision of professor Jan Koenderink and Sylvia Pont. In the end of 2008 the group was transfered to Delft University of Technology, the faculty of Industrial Design under the supervision of professor Huib de Ridder.